Aus dem Rudolf-Virchow-Zentrum Würzburg

Forschungszentrum für Experimentelle Biomedizin der Universität Würzburg

Leiterin und Leiter: Prof. Dr. Caroline Kisker und Prof. Dr. Bernhard Nieswandt

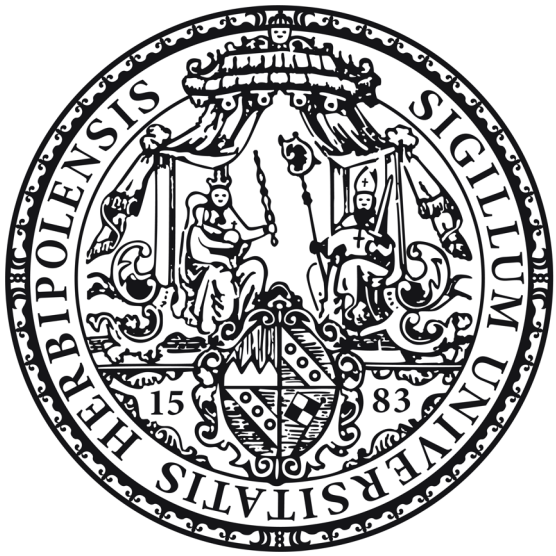

The Role of Protein Kinase D 1 in the regulation of murine adipose tissue function under physiological and pathophysiological conditions

Die Bedeutung von Protein Kinase D 1 in der Funktion von murinem Fettgewebe unter physiologischen und pathophysiologischen Bedingungen

Inaugural – Dissertation

zur Erlangung der Doktorwürde der

Medizinischen Fakultät

der

Julius-Maximilians-University Würzburg

Vorgelegt von

Anja Maria Slotta

aus Aachen

Würzburg, März 2018

Referentin: Prof. Dr. rer. nat. Antje Gohla

Koreferent: Prof. Dr. med. Martin Faßnacht-Capeller

Dekan: Prof. Dr. Matthias Frosch

Tag der mündlichen Prüfung: 05.04.2019

Die Promovendin ist Ärztin

Meinem Vater

Table of Contents

1 Introduction

1.1 Adipose tissue

Adipose tissue consists of adipocytes which are cells specialized in storing large quantities of energy found in vertebrates [1]. Each adipocyte is surrounded by connective tissue of basal lamina, reticular and collagen fibers that hold the cells together as connective tissue. Segments of adipose tissue are provided with nerves and blood vessels which ensure communication with other cells and tissues of the human body [2]. Depending on the gender, age and health status the content of adipose tissue in the body can vary from approximately 6% in man athletes to more than 32% in obese individuals [3]. Despite acting as an energy storage adipose tissue fulfils several important functions in the organism. Adipocytes contribute to the maintenance of core body temperature, hormonal homeostasis and serve as a mechanical protection for other organs [1].

1.1.1 Types of adipose tissue

There are three different types of adipose tissue distributed differently throughout the body: White adipocytes, which make up the highest amount, brown, and beige adipocytes.

The localization of white adipose tissue (WAT) in the human body distinguishes part of its function [1]. The main function of calorie storage and energy homeostasis is met by subcutaneous and visceral WAT [2]. However, subcutaneous WAT was found to have protective benefits on glucose homeostasis, insulin sensitivity, and triglyceride plasma levels whereas WAT located intra-abdominal (visceral) appears to negatively affect metabolism [4]. Furthermore, subcutaneous adipose tissue serves as isolator from temperature changes in environment and protects from loss of body heat. Depots of adipose tissue also cushion important parts of the body exposed to high mechanical pressure such as the heel. Additionally, fat depots ensure the position of organs e.g. eyes in the orbita, kidneys in the renal bed, and coronary vessels around the heart. These depots of adipose tissue are only reduced under extreme nutritional deficiency conditions such as malnutrition or cachexia resulting from cancer disease [2].

In humans, depots of brown adipose tissue (BAT) can be found predominantly in infants. Their ability to produce heat through nonshivering thermogenesis presumably is an evolutionary advantage after birth. Although for a long time it was assumed that BAT disappears with adulthood, new evidence was found that it only diminishes with age [1, 5]. ^{18}F-FDG-PET/CT scans revealed remaining BAT at supraclavicular, cervical, axillary and spinal locations of human adults which could be verified in tissue biopsies [6]. Moreover, BAT in human adults can be activated by exposure to cold. A correlation between its activity and low body mass index (BMI) as well as body fat in human adults was described [7, 8]. In comparison, rodents exhibit interscapular and perirenal depots of BAT at all ages [1, 5].

Certain histological differences distinguish white from brown adipocytes. In adipocytes, fat accumulates in lipid droplets surrounded by a phospholipid layer containing perlipin-1 which forms a vacuole separated from other cell organelles. While white adipocytes rather appear with one vacuole, brown adipocytes contain many smaller lipid droplets [2, 9]. Furthermore, brown adipocytes display a high density of mitochondria that lay the basis for their function: The inner mitochondrial membrane contains uncoupling protein-1 (UCP-1), a protein expressed specifically in brown adipocytes [1, 2, 9]. UCP-1, also called thermogenin, is responsible for thermogenesis by BAT. While the respiratory chain in mitochondrial membrane generates a proton gradient necessary to produce energy in form of ATP, UCP-1 establishes a back current for protons. Therefore, it uncouples the mechanism of respiratory chain and produces energy in form of heat. Stimulation of the sympathetic nervous system and catecholamine secretion in BAT induce increase of intracellular cyclic adenosine monophosphate (cAMP)-levels and lipolysis (detail in 1.1.2). Free fatty acids that are generated by lipolysis metabolize in mitochondria and its products are important for respiratory chain. Additionally, high cAMP concentration leads to transcription of UCP-1 and therefore enhance production of heat [10]. Hence, BAT

dissipates calories, therefore changes energy equation, and could possibly protect from obesity, as shown in mice [11].

Recent findings revealed the existence of another type of adipocytes, so called beige or bright adipocytes. They occur mainly within subcutaneous WAT but show multiple lipid droplets, high density of mitochondria, and expression of UCP-1 with the same function in heat production as in brown adipocytes. Although the origin of beige adipocytes is controversially discussed, they appear to develop from white adipocytes by induction with PPARγ-agonist, adrenergic stimulation, exercise, or cold exposure. This process is called “browning” or “beiging” of WAT. Similar to brown, beige adipocytes possess a large number of mitochondria and express UCP-1, which allows them to dissipate energy in the form of heat [1, 5, 12]. However, recently a novel mechanism of heat dissipation utilized primarily by beige adipocytes has been proposed. Proteomic study revealed that beige adipocytes possess creatine enzyme driven substrate cycle that enhances thermogenesis. Creatine drives energy dissipation by mitochondria of beige adipocytes by accepting phosphate group from ATP and its subsequent release in the process mediated by phosphatase PHOSPHO1. The same study showed that this process contributes largely to the total energy balance in rodents and possibly also in humans [13].

1.1.2 Physiology of white adipocytes

In vertebrates, adipocytes have an evolutionary important function and lay the basis for survival of living organism: They store energy at times of nutritional abundance through lipogenesis in lipid vacuoles and provide the organism with energy through lipolysis when in nourishment deprivation. Therefore, adipose tissue is the main organ to balance energy homeostasis next to the liver and the intestines [1, 14].

Lipid droplets in adipocytes consist of triacylglycerides (TGs) stored without water. Therefore TGs have a higher energy density than carbohydrates, which are stored as glycogen with water in liver and muscles [9]. Lipolysis, the process of breaking down

TGs, is induced during fasting or can be stress mediated, promoted by several hormones among which catecholamines are of greatest importance. Variables such as inflammation, oncological, genetic, metabolic and endocrine diseases, can alternate the rate of lipolysis [14]. Three enzymes, adipose triglyceride lipase (ATGL), hormone-sensitive lipase (HSL), and monoacylgycerol lipase (MGL) hydrolyze TGs in adipocytes to release diacylglycerol (DAG) first, then monoacylglycerol, at last glycerol and in each step free fatty acids (FFA) [15]. However, when ATGL and HSL are deactivated lipolysis is reduced to 2 percent of the regular lipolysis rate in WAT of mice, indicating that they display main enzymes for FFA release [16]. FFAs are released to circulation to provide needy organs with energy. They either undergo β-oxidation in mitochondria, which products are necessary for the citric acid cycle and the respiratory chain, or are metabolized to ketone bodies in liver cells. Thus, adipocytes provide energy for all cells in the body [10, 14].

However, in time of food abundance adipocytes adapt by storing calories in form of TG in the process of lipogenesis. TGs are synthesized from fatty acids and glycerol with monoacylglycerolphosphate and 1,2-diacylglycerol as intermediate steps [10]. There are two ways to expand capacity for fat deposition: First, by hypertrophy of cells and second, due to a limit in adipocyte size by hyperplasia in the process of adipogenesis. Although this mechanism is important for organisms survival, it is also the basis for obesity. Interestingly, loss of body weight leads to reduction of cell size but not cell number [1].

Energy homeostasis in an organism needs to be tightly controlled and adipocytes play a pivotal role in its regulation. After food intake, pancreatic β-cells secrete insulin that promotes glucose uptake from blood into muscle cells and adipocytes. This means that adipocytes need to be sensitive to insulin in order to balance glucose blood levels [9].

Additionally, adipocytes act as an endocrine organ and secret adipokines which regulate food consumption, energy expenditure, and also peripheral insulin sensitivity. One prominent adipokine is leptin. It has anti-hyperglycaemic effects, stimulates energy expenditure while lowering food intake via the hypothalamus. It also promotes

inflammation and has complex effects on bone remodeling [1]. Loss of function due to mutations in leptin and the leptin receptor result in obesity [17].

Adiponectin is another adipokine produced by adipocytes. Adiponectin has positive effects on metabolic health by improving β-cell function together with insulin sensitivity, serum lipid levels and inducing metabolization of fatty acids in the liver [18].

Further adipokine, resistin promotes insulin resistance in mice models and studies show high levels of resistin in obese mice. However, mechanisms of its action and its impact on metabolism of humans has not been fully elucidated so far [19].

Furthermore, the sympathetic innervation of fat tissue makes lipolysis possible. Fasting induced by drop of blood glucose level as well as cold exposure lead to secretion of catecholamines epinephrine and norepinephrine. These bind to β-adrenergic receptors located at adipocyte cell membrane and activate a signaling cascade to increase lipolysis [20]. On the other hand, parasympathetic nerves are stimulated after feeding and enhance lipid accumulation [21]. Apparently, visceral fat is more densely innervated than subcutaneous fat [20].

1.1.3 Pathophysiology of obesity

Adipocytes play a pivotal role in development of metabolic diseases as abnormal and excessive TG accumulation in these cells result in obesity [22]. Globally speaking, obesity is caused by an imbalanced energy equation resulting from an increased energy intake of high caloric foods as well as insufficient caloric expenditure of the body via physical activity, basal metabolism, and adaptive thermogenesis. Genetic, environmental, and psychological factors influence this equation [22, 23]. In clinical means, obesity is classified using the Body Mass Index (BMI, [kg/m^2]), which is calculated by the person's weight (in kilogramm) and divided by the square of the person's height (in meters). According to WHO, BMI of 30 and more counts as obesity. In 2016, the WHO estimated over 650 million adults (18 years and above), 13 percent of the population worldwide, to be obese. More importantly, 41 million children under 5 years old were found to be obese or overweight (BMI equal or greater than 25) in

2016, which is associated with their future obesity, disability, and premature death next to acute health impediments and increased risk for insulin resistance, amongst others [23].

Central obesity due to an increased amount of white adipose tissue in the abdomen is the main component of the metabolic syndrome [24]. The International Diabetes Federation (IDF) defines the metabolic syndrome as abdominal obesity, specifically meaning waist circumference of 94 cm or more for European men and 80 cm or more for European women excluding other ethnicities with different values, combined with two of the following aspects: raised TG levels, reduced HDL (high-density-lipoprotein-cholesterol) levels in blood, raised blood pressure, or treatment of any of those three factors, raised fasting plasma glucose levels or previously diagnosed type 2 diabetes mellitus (T2DM) [24]. Emphasis is put on the factor abdominal obesity, which is associated especially with development of T2DM but also with the other risk factors listed in the definition of metabolic syndrome. Low HDL cholesterol and elevated TG blood levels can be summoned as atherogenic dyslipidaemia, which is found in humans with metabolic syndrome and T2DM. The link between each listed risk factor is complex but they are most important for development of cadiocascular disease. It is generally accepted that the metabolic syndrome is a combination of the most dangerous risk factors to cause heart attack or stroke [24]. In fact, the World Health Organization (WHO) listed ischaemic heart disease with 8.67 million deaths as the first leading cause for death worldwide in the year 2015, followed by stroke with 6.24 million deaths as the second leading cause, and diabetes mellitus (DM) on the sixth place [25]. Most importantly, the number of deaths caused by DM increased from less than 1 million in 2010 to 1.59 million in 2015 [25]. Hence, metabolic syndrome and diseases associated with it form a big threat for the well-being of our society.

T2DM is a metabolic disease characterized by chronic hyperglycaemia caused by a composition of peripheral insulin resistance, impaired insulin secretion and apoptosis of pancreatic β-cells, elevated glucagon secretion by pancreatic α-cells, and impaired

incretin secretion as well as incretin effectiveness [26]. According to WHO, T2DM is a result of overweight and physical inactivity [27]. The great majority of T2DM develops on the basis of metabolic syndrome. Approximately 80 percent of people with T2DM are overweight. This makes maintenance of normal body weight and reduction of body weight in obese one of the best preventive courses of action [26].

As in obesity white adipocyte hypertrophy and hyperplasia progresses, adipose tissue can eventually outgrow its blood supply which causes hypoxia in the tissue [1]. This leads to macrophage invasion and cytokine secretion, including TNF-α (tumor necrosis factor α), resistin, MCP-1 (macrophage chemoattractant protein-1) and others, and in essence to inflammation in WAT. In addition, fibrosis may develop, which supports inflammatory progress [9]. Pro-inflammatory cytokines were found to negatively affect insulin sensitivity not only in adipocytes but also in liver and muscle [1]. However, an other study proposed that increase of fibrosis in adipose tissue restricts adipocyte hypertrophy, which is beneficial for metabolic health and is therefore protective against T2DM [28]. In addition to the inflammatory process, adipocytes endocrine function alters in obese individuals and contributes to decreased insulin sensitivity. Secretion of adiponectin for instance decreases with gain of visceral fat and therefore its positive effects on insulin sensitivity diminish in obese individuals. Resistin levels on the other hand are increased in obese mice and cause elevated insulin resistance in them. Although leptin is helpful in reducing body weight (1.1.2), it also enhances cytokine production and therefore stimulates inflammation. Leptin blood levels correlate with mass of fat [1, 9, 22]. All in all, these mechanisms show that chronic inflammation is associated with obesity and inflammation results in peripheral insulin resistance and eventually in T2DM [29]. Insulin resistance in adipose tissue leads to release of FFA into blood circulation [9]. When reaching liver, FFA induce elevation of LDL (low density lipoprotein cholesterol), apolipoprotein B and TG whereas HDL is reduced. This atherogenic dyslipidaemia significantly increases not only the risk for heart disease but in addition, chronic increased FFA blood levels induce decrease of insulin secretion and therefore causes insulin resistance in liver and other tissues, too – a vicious cycle [9, 24].

Prevalence of DM in 2014 was 8.5 percent among adults worldwide and the majority suffered from T2DM. Consequences of DM include high risk of death from cardiovascular disease, in detail heart attack and stroke, risk of neuropathy and reduced blood flow, which can result in lower limb loss, and risk of retinopathy and kidney failure [27].

Apart from metabolic disease, obesity is associated with development of certain cancer types such of endometrium, breast, colon, renal, esophageal, and pancreatic cancer [1, 23].
Thus, it is of great importance for the future of human global health to promote research and investigate possibilities to prevent and fight obesity, T2DM, and metabolic syndrome, all of which are linked to adipocyte function.

1.2 Protein kinase D 1

PKD1 belongs to a group of isoforms in the protein kinase D (PKD) family of serine/threonine kinases [30]. The PKD family is classified in the calcium/calmodulin-dependent protein kinases (CAMKs) superfamily due to similarities of the kinase domain. There are three different isoforms of PKDs in mammals with different tissue and cell expression: PKD1 (also referred to as PKCμ), PKD2, and PKD3 (also: PKCv) sharing a similar modular structure but encoded in three different genes. PKDs exhibit an N-terminal regulatory domain containing two cystein-rich zink-finger motifs (cysteine-rich domain, CRD) and an autoinhibitory pleckstrin homology (PH)-domain. More specifically, the CRD binds to diacylglycerol (DAG) and phorbol esters to translocate the kinase to plasma membrane and nucleus and has an inhibitory effect on the kinase catalytic activity. Mutation of PH-domain or deletion of zink-fingers from the CRD lead to fully active PKD function. Thus, the N-terminal domain is involved in intramolecular inhibition of PKDs catalytic activity [30, 31].

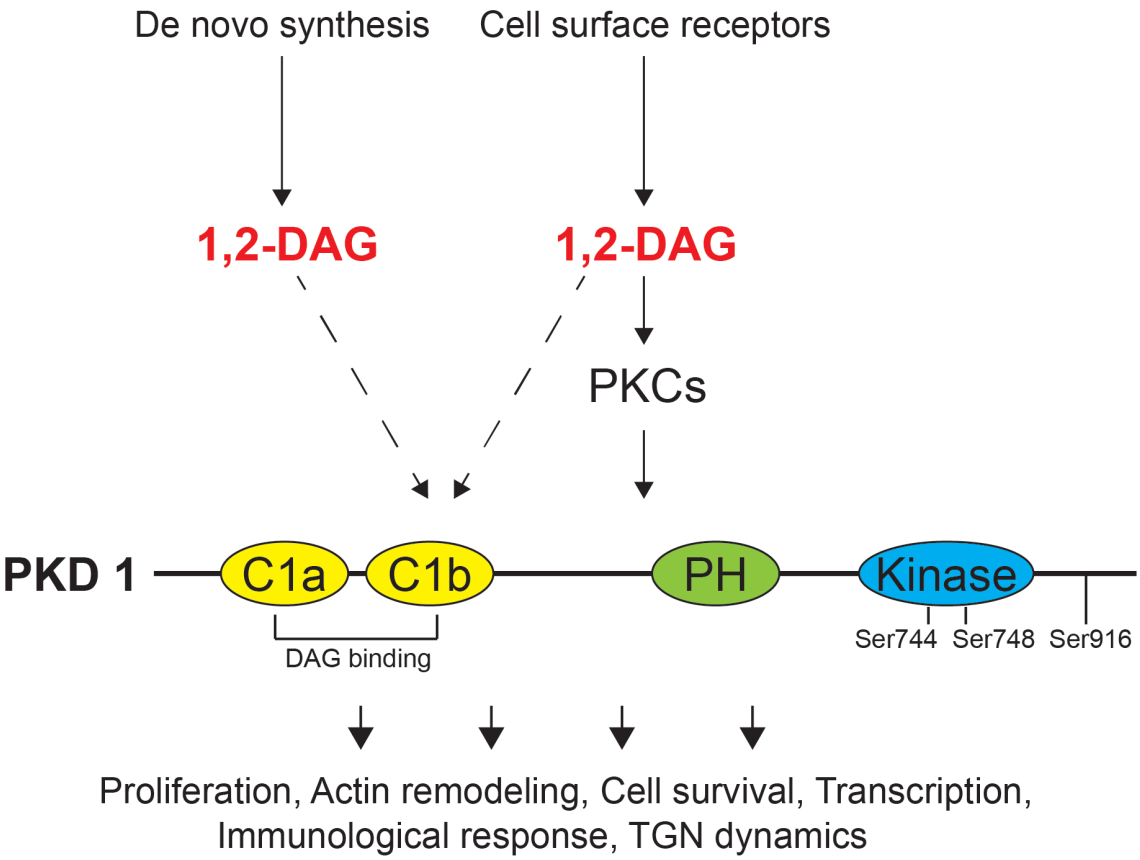

Figure 1: Signalling pathway and modular structure of PKD1 in mice. 1,2-DAG derived either from cell surface receptor stimulation (GPCR, TKR) via Phospholipase C activation or from de novo synthesis of TG can bind PKD1 and PKC. To activate PKD1, PKC phosphorylates PKD1 at Ser744 and Ser749, and PKD1 auto-phosphorylates at Ser916. Activated PKD1 can then execute its biological functions. 1,2-DAG, 1,2-Diacylglycerol; PKC, Protein Kinase C; PKD1, Protein Kinase D1; C1a and C1b, first and second cystein-rich Zn-finger domain in CRD that bind DAG; PH, pleckstrin homology domain; Kinase, Kinase domain; Ser744, Ser748 and Ser916, serine phosphorylation sites. Figure was kindly provided by G. Sumara and M. Löffler.

Furthermore, there is a C-terminal kinase domain, which can be phosphorylated and therefore activates the kinase. PKD1s kinase domain can be phosphorylated by DAG-activated Protein Kinase C isoforms (PKCs δ, ε, η, θ) at its serines in the activation loop, Ser-744 and Ser-748 in murine PKD1, which is necessary for the kinases activity [31]. It has been shown that on the one hand mutation at Ser-744 and Ser-748 leads to inability of PKD1 activation, on the other hand imitation of phosphorylation through mutation at these sites creates a constitutively active kinase [32]. Additionally, PKD1 has the ability to auto-phosphorylate Ser-916 (pSer-916, in murine PKD1) at the far C-terminal end for conformational changes in PKD1. For this step, phosphorylated Ser-

744 (pSer-744) is required, and furthermore, pSer-916 is necessary for auto-phosphorylation of Ser-748. Therefore, PKDs activity can be traced by using antibodies against pSer-744/748 or against pSer-916 [30]. Of note, that these phosphorylation sites apply for mice and differ from human PKD1 (Ser-738/Ser-742 in activation loop and Ser-910 at far N-terminal end) [33].

There is a pool of PKD1 located mainly in the cytosol of resting cells. Upon G-protein coupled receptor (GPCR) or tyrosine-kinase receptor (TKR) stimulation of cells, Phosolipase C (PLC) is activated leading to the generation of DAG at the plasma membrane to bind and activate PKC, (Figure 1) [30]. Study showed that the 1,2-DAG stereoisomer fulfills activation of PKC, which is provided by PLC-pathway at plasma membrane [34].

As mentioned before, PKDs use the CRD for translocation in cells. Therefore, PLC-produced DAG also binds to PKDs second zink-finger domain in CRD (C1b). It then translocates via the second zink-finger domain to the plasma membrane. Attached to the plasma membrane, activated PKC phosphorylates PKD in the activation loop at Ser-744 and Ser-748. This step is needed to activate PKD which then rapidly dissociates from the plasma membrane to further cross the nucleic membrane again by using the second zink-finger and accumulate in the cell nucleus. For export from the nucleus the PH-domain is required.[30, 31]

Yet, PKD isoforms can be activated at other subcellular location. The first zink-finger domain (C1a) of CRD determines PKDs translocation into the trans-Golgi network (TGN) [30]. Importantly, this step is dependent on local synthesis and levels of DAG binding to PKD1 [35]. Of note, PKD isoforms regulate TGN dynamics and are required for vesicle fission from the TGN [36].

Hypothetically, 1,2-DAG produced as an intermediate product during local triglyceride synthesis in the endoplasmic reticulum (ER) potentially also activates PKC and PKD, however, this should be further analyzed [15].

Hence, PKD1 is activated by DAG-PKC-pathway and DAG regulates localization of PKD1. PKD1 is located within the cell cytosol, TGN, nucleus, and mitochondria and can be

activated via the PKC-pathway in vivo through neuropeptides, purinergic receptor activation, growth factors, neurotensin and many more, next to DAG and phorbol esters [30, 31, 36, 37]. Specific substrates and changes in sub-cellular localization determine its function and the resulting biological effect [38].

However, PKD also displays PKC-independent pathways for activation. A Src-Abl-pathway mediates phosphorylation of PKD1 at the PH-domain through the action of tyrosine [37]. Moreover, PKD1 is a substrate of caspase-3 and is regulated in apoptosis, during which cleavage of PKD1 at two sites showed increase of the kinases activity [39]. M3-muscarin receptors were also shown to activate PKD1 in pancreatic β-cells via direct phosphorylation in a β-arrestin-dependent manner [40].

Recently, Chang et al. demonstrated that stimulation with GPCR agonists induces phosphorylation of PKD1 at Ser-203 in the N-terminal end. The study identified group I p21-activated kinase (PAK) as novel upstream kinase to phosphorylate Ser-203 and activate PKD1 in an PKC-independent manner. They showed that this mechanism leads to translocation of PKD1 into the nucleus where it regulates HDAC5 localization and phosphorylation [41].

Thus, not all possibilities of PKD1 regulation and activation can be explained by the PKC-pathway and are yet to be found.

Moreover, previous studies performed by M. Loeffler et al. implicated PKD1 in regulation of a number of cellular and physiological processes influencing body weight, composition and nutrient metabolism

1.2.1 Function of PKD1

PKD1 exhibits a variety of biological functions dependent on the cell type, substrate, and intracellular localization (plasma membrane, trans-Golgi Network, nucleus, mitochondria). Many different processes on cellular level were shown to incorporate PKD in regulation of proliferation, differentiation, cell motility, apoptosis, gene expression, intracellular signal pathways, and trans-Golgi Network dynamics [36-38, 42].

Proliferation

PKD1 supports proliferation and differentiation of cells, either on normal or abnormal level, meaning cancer progression. For example, fibroblasts stimulated with Gq-receptor agonist induce mitogenesis of fibroblasts via PKD1 activation [38]. More detailed, Gq-receptor-mediated activation of PKD enhances ERK signaling in MEK/ERK/RSK (MEK, ERK kinase; ERK, extracellular-regulated protein kinase; RSK, ribosomal s6 kinase) pathway and therefore potentiates DNA synthesis in these cells [43]. In epidermal keratinocytes, PKD1 is more expressed during proliferation but lower during differentiation of keratinocytes [44]. In these cells, the proliferative effect of PKD is also attributed to activation of ERK-pathway and enhanced DNA synthesis [45]. Regulation in differentiation processes by PKD1 were shown in osteoblasts and formation of bone [38]. Moreover, PKD1 plays an important role in angiogenesis, a process supporting tumor growth, obesity and cardiovascular development. It was shown that vascular epithelial growth factor (VEGF)-stimulated endothelial cells need PKD1 signaling for further gene and DNA synthesis and proliferation [46].

Cell migration

Furthermore, PKD1 is involved in motion and migration of cells by interacting with actin cytoskeleton in various aspects. Active slingshot phosphatase (SSH) family member SSH1L binds to filamentous actin (F-actin), dephosphorylates and therefore activates cofilin (F-actin depoymerization and severing factor ADF/cofilin) inducing F-actin polymerization and cell migration. Active PKD1 co-localizes with SSH1L to F-actin, phosphorylates and inactives SSH1L and therefore inhibits F-actin reorganization and cell motility [47]. Furthermore, PKD1 interrupts F-actin remodelling by phosphorylating RIN1 (Rab interactor-1) and cortactin [48, 49].

Moreover, PKD1s phosphorylation of E-Cadherin enhances cell-cell adhesion and inhibits cell motion. Interestingly, expression of both proteins is diminished in certain cancer types leading to advanced invasiveness of cancer cells [36, 50].

Oxidative Stress and Apoptosis

Oxidative stress was also shown to activate PKD1 through the Src-Abl tyrosine kinase pathway that phosphorylates the PH-domain in addition to phosphorylation at the PKD activation loop through PKC. Fully activated PKD1 in turn activates nuclear factor κB (NF-κB), a transcriptional factor that protects from oxidative-stress-induced cell death, through the action of IκB-kinase β (IKKβ) of the IKK-complex [37, 51]. In neurodegenerative diseases, PKD1 was identified as a key kinase to support cell survival and protect neurons from oxidative stress, which was also attributed to PKC-dependent phosphorylation in PKD1s activation loop [52]. Moreover, in cardiomyocytes activation of PKD1 was shown to be mediated by RhoA, a guanosine triphosphatase activated by GPCR leading to PLCε activation and generation of DAG. Active PKD1 phosphorylates and therefore inhibits SSH1L in cardiomyocytes, which diminishes oxidative-stress induced translocation of cofilin 2 to mitochondria, protecting mitochondrial membrane and promoting cell survival [53]. Thus, PKD1 supports survival of cells under oxidative stress and has anti-apoptotic attributes [36, 37].

PKD1 in regulation of transcription

PKD1 was also shown to regulate transcription. Specifically, PKD1 phosphorylates specific sites of class II histone deacetylases (HDAC), which suppress transcription. PKD1-dependent phosphorylation of members of class II HDACs (HDAC4, HDAC5 and HDAC7) promotes its dissociation from the chromatin and nuclear export and therefore promotes transcription of the target genes [37]. This mechanism is especially important in regulation of heart remodeling after hypertrophic stimuli. Mice deficient for PKD1 specifically in cardiomyocytes, are partially resistant to pathological heart remodeling due to the enhanced nuclear localization of class II HDACs which suppress transcription of key genes mediating pathological heart remodeling [54]. Furthermore, PKD1 was found to enhance transcriptional activity through phorphorylation of cAMP-response element-binding protein (CREB) [55]. In the context of heart remodeling CREB was identified as a substrate of PKD. This PKD-CREB phosphorylation pathway

leads to activation of CRE-responsive promotor in nuclei of cardiomyocytes, suggesting participation of PKD in cardiac remodeling [56].

Immunological response

Also in B and T lymphocytes PKD shows regulatory involvement in immunological responses. PKD is activated and changes localization from cytosol to cell membrane when antigen receptors are stimulated in pre-T cells. Depending on localization in pre-T cells, PKD induces their proliferation and differentiation [57]. Furthermore, PKD1 was shown to be part of signaling cascade that recruits neutrophils into inflammatory sites. In mice, p38 mitogen-activated protein kinase (MAPK) p38δ enhances chemotaxis and recruitment of neutrophils and (as in pancreatic β-cells [42], see below) has inhibitory effects on PKD1 activity in neutrophils. Here, PKD1 phosphorylates p85α, a regulatory subunit of phosphoinositide 3-kinase (PI3 kinase), increasing its binding to and activity of PTEN (phosphatase tensin homologue) that in turn diminishes neutrophil migration. Hence, inhibition of PKD1 by MAPK p38δ enhances neutrophil recruitment and migration [58]. Also, PKD was found to be part of immune response signaling of toll-like-receptors of macrophages, bone marrow derived mast cells, and epidermal cells [38].

PKD1 is a master regulator of trans-Golgi Network (TGN) dynamics

At the TGN PKD1 activity is required for fission of vesicles acting as carries between TGN and plasma membrane [59]. Additionally, PKD1 is involved in cell secretion, for instance of aldosterone and cortisol from adrenocortical cells, or of insulin from pancreatic β-cells [38]. Moreover, in pancreatic β-cells PKD1 activity is subjected to the control of other stress activated kinase, namely MAPK p38δ, which inhibits its activation and suppresses insulin vesicle fission from TGN. Consistently, PKD1 is pivotal in carbachol (mimicking parasympathetic stimulation) and glucose stimulated insulin secretion from pancreatic β-cells. Deletion of PKD1 in these cells results in inhibited insulin secretion upon glucose stimulation. Accordant with that, PKD1 is activated by deletion of p38δ which leads to improved glucose tolerance by enhanced insulin secretion [42]. Furthermore, PKD is involved in insulin granule degradation in β-cells

and PKDs activity decreases at the TGN upon starvation of these cells suggesting that nutrients regulate PKDs activity [60]. It was also demonstrated that PKD1 is required for glucose-stimulated insulin secretion via G-protein receptor (GPR) 40 upon stimulation with fatty acids in murine islets [61]. All of these findings make PKD1 an interesting topic in research on DM and metabolic diseases.

Cancer

PKD1s multiple functions in fundamental cellular processes are associated with development of cancer. However, classification in positive or negative effects of PKD1 expression on cancer disease depends on tissue and cancer cell type [38, 62].

In breast as well as gastric cancer, PKD1 expression was found to be downregulated due to epigenetic hypermethylation of PKD1s promoter region [63, 64]. Furthermore, upregulation of PKD1 inhibits invasiveness and metastasis of breast cancer through decrease of cell migration via phosphorylation and inactivation of slingshot phosphatase 1L (SSH1L), phosphorylation of cortactin, and phosphorylation of Ras and RIN1 [62]. Also, PKD1 activity inhibits expression of pro-invasive matrix metalloproteinases (MMP) in breast as well as prostate cancer cells [62, 64]. Additionally, PKD1 activity in breast and prostate cancer regulates epithelial-mesenchymal-transition (EMT) through phosphorylation of transcription factor Snail (SNAI1) at Ser-11, which leads to E-cadherine expression, and therefore preventing EMT process [64, 65]. However, other studies indicate that upregulation of PKD1 has a pro-oncogenic effect on prostate cancer development [62]. In pancreatic cancer cells overexpression of PKD1 was observed to promote cancer progress through neurotensin-induced synthesis of DNA via MAPK/ERK kinase 1 and ERK2 [66]. Importantly, inhibition of PKD1 and PKD2 was shown to reduce pancreatic tumor growth and to be a potential target for pancreatic tumor therapy [67].

1.2.2 Role of PKD1 in mouse adipose tissue

As mentioned above, adipocytes play a pivotal role in development of metabolic diseases (1.1.3). To investigate factors influencing development of obesity other than disadvantageous life-style, multiple approaches were used to understand the impact

of heritability, specifically genetic and epigenetic influence on obesity and T2DM. A genome-wide association study implicated that common genetic variation can cause approximately 21 percent of BMI variation in humans [68]. Using genome-wide significance single nucleotide polymorphisms (SNP), this study investigated the link between gene-loci and BMI and identified 97 loci that account for 2.7 % variance in BMI phenotype. Of these, protein kinase D1 (PKD1) was found as a novel gene-locus associated with BMI [68].

Previous studies perfomed by Mona Löffler in the G. Sumara research group revealed that PKD1 plays a pivotal role in regulation of adipocyte function. It is of notice that PKD1 is predominately expressed in subcutaneous (subWAT), epigonadal (epiWAT), and isolated white adipose tissue among other cell types of mice with highest expression in epiWAT (Figure 2).

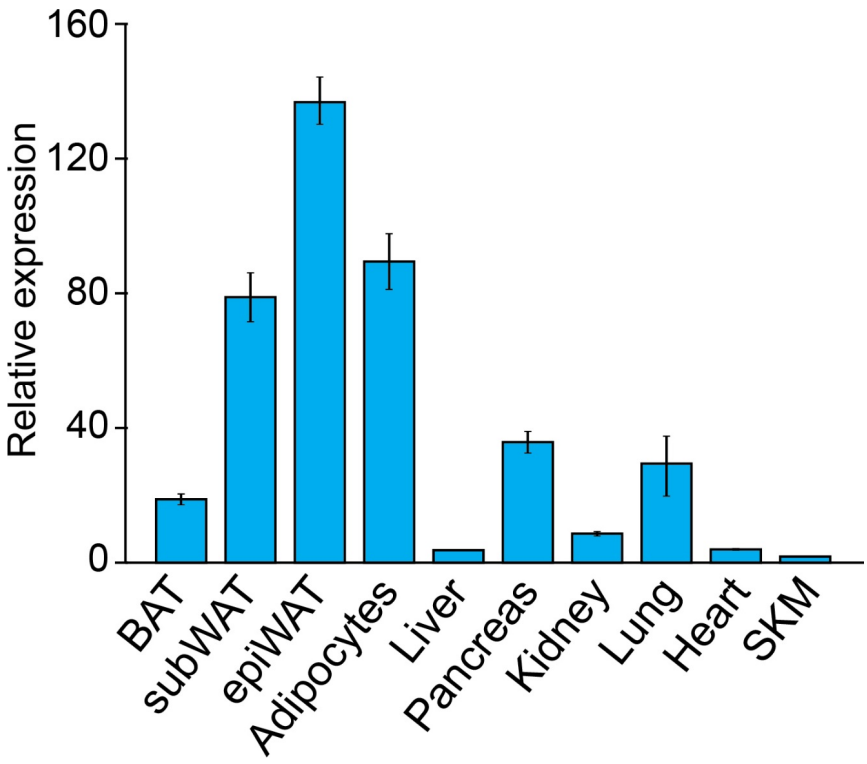

Figure 2: Mona Löffler et al., unpublished. PKD1 is predominantly expressed in white adipose tissue of mice. qPCR was conducted to determine relative expression of PKD1 in different tissues of regular black-6 mice (n=4). Brown adipose tissue (BAT), subcutaneous (subWAT) and epigonadal white adipose tissue (epiWAT), isolated adipocytes, liver, pancreas, kidney, lung, heart, and skeletal muscle (SKM) were investigated.

This specific pattern of expression of PKD1 prompted the G. Sumara research group to generate mice deficient for PKD1 specifically in adipocytes (PKD1adipo. Δ/Δ) by using PKD1flox/flox mice [54] and adiponectin promotor-driven Cre mice [69].

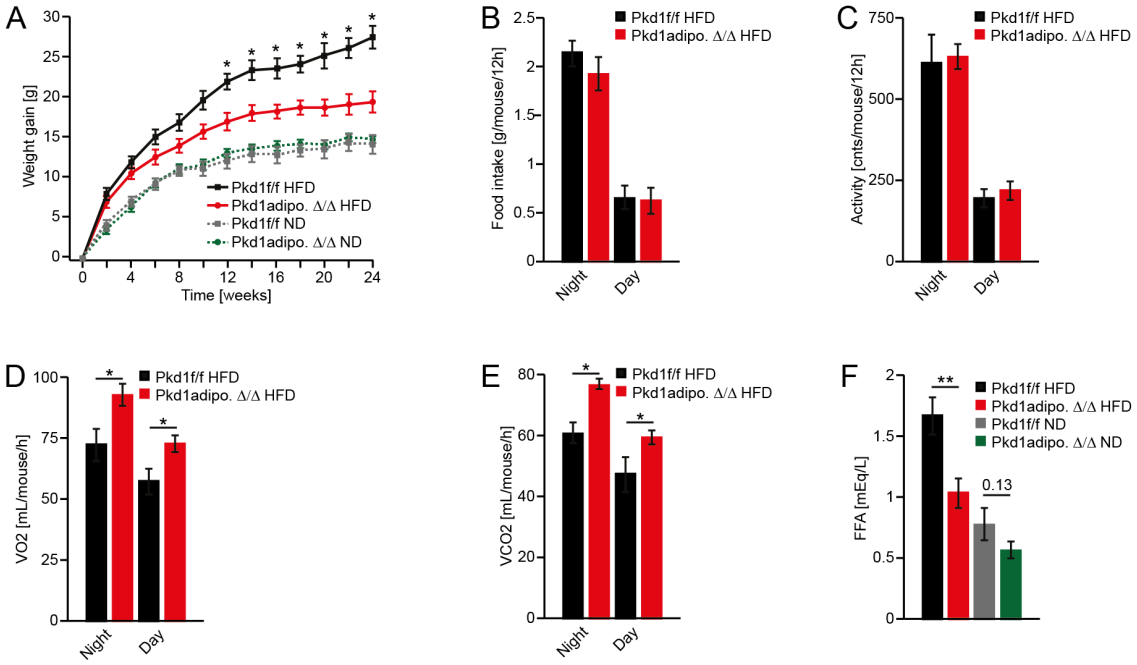

Figure 3: Mona Löffler et al., unpublished. PKD1 deficiency in adipose tissue protects from high fat diet-induced obesity. Body weight gain (A) over 24 weeks of HFD or ND in mice expressing (PKD1flox/flox, wt) or deficient (PKD1adipo. Δ/Δ, ko) for PKD1 in adipose tissue. Food intake (B), mouse activity (C), O_2 consumption (D), CO_2 dissipation (E) and peripheral FFA-blood levels (F). Data for A - E was collected with PhenoMaster, data for F was determined with NEFA-HR(2) reagent (by Wako). For A and F n=10 wt mice and n=8 ko mice were used for HFD, and n=5 wt mice and n=10 ko mice were used for ND; For B-E n=7 animals were analyzed. Data is presented as mean ± SEM. For all data, *p < 0.05 and **p < 0.05, using two way ANOVA with Tukey's multiple comparisons post test and unpaired, two-tailed Student's T-Test.

PKD1-deficient mice gained significantly less weight when fed with high fat diet (HFD) than wildtype mice, however, their weight was not altered when fed normal chow diet (ND, Figure 3, A). The data G. Sumaras research group generated indicate that PKD1adipo. Δ/Δ mice are partially resistant to HFD induced obesity.

Body weight is a result of the energy balance of the organism. In other words relative increase of the amount of the energy ingested over the amount of energy dissipated results in increase in body weight, conversely negative energy balance results in body weight loss [9]. Hence, in living organism, energy intake can be measured with the individuals' food intake but must be evaluated in relation to the energy dissipation

[22]. However, energy can be dissipated by the organism in different forms. Primarily, organisms utilize the energy ingested to sustain basal metabolism of all the cells in the body. Energy can also be utilized by the organism for physical activity as well as sustaining optimal core body temperature in the process of adaptive thermogenesis [22]. To test all of these possibilities, G. Sumara research group placed PKD1$_{adipo.\ \Delta/\Delta}$ mice in the Phenomaster metabolic cages which allows simultaneous assessment of the food intake, voluntary movements (activity), O_2 consumption and CO_2 dissipation in living mice. PKD1$_{adipo.\ \Delta/\Delta}$ mice presented normal food intake (Figure 3, B) and voluntary movements (Figure 3, C) compared to wild-type littermates when fed with HFD. However, deficiency of PKD1 specifically in adipocytes resulted in increased O_2 consumption and higher CO_2 dissipation (Figure 3, D and E) indicating elevated energy expenditure in these animals.

Adipocytes are the main regulators of lipid levels in the circulation (1.1.2). As mentioned above, adipocytes secrete FFA in the process of lipolysis [14]. Of note, PKD1$_{adipo.\ \Delta/\Delta}$ mice present reduced FFA levels compared to the control mice when fed with HFD (Figure 3, F). This indicates that PKD1 might promotes lipolysis or/and suppresses FFA oxidation in adipocytes or in other peripheral organs.

Since the levels of adipokines leptin and adiponectin are not changed in PKD1$_{adipo.\ \Delta/\Delta}$ mice fed HFD (unpublished data generated by M. Löffler et al.) and physical activity of mice is not altered by deletion of PKD1, we postulate that mice deficient for PKD1 specifically in adipocytes present increased energy expenditure due to the enhanced metabolic activity of adipocytes.

However, the precise mechanism of PKD1-dependent regulation of energy expenditure and FFA levels are not known. Also, the physiological conditions when PKD1 is activated were not yet identified in adipocytes. For these reasons, PKD1 and its impact on regulation of metabolic homeostasis is subject of this study.

1.3 Aim of the study

In adipose tissue, imbalance of energy homeostasis by excessive energy intake over energy dissipation and excessive TG accumulation in these cells results in obesity, and eventually in development of metabolic diseases [1, 14, 22]. PKD1 is involved in regulation of many diverse physiological and pathophysiological processes in vertebrates [30, 36-38, 62], (1.2.1). However, the role of PKD1 in adipocytes physiology and pathophysiology has not been fully understood. Also, physiological mechanisms regulating PKD1 in adipocytes are still not known.

Therefore, this study focused on three specific goals: The first one was the identification of physiological conditions that regulate PKD1 protein levels, PKD1 expression, and its activity in murine adipocytes. The response of PKD1 in murine adipose tissue to feeding and fasting of mice, and further analysis of the response to stimulated lipolysis in white adipocytes were in focus. In other experiment, silencing of ATGL was used to distinguish effect of lipolysis and its products on PKD1 from effect of direct stimulation of adipocytes with isoproterenol at inhibited lipolysis in these cells. Furthermore, the condition of over-nutrition and its influence on PKD1 expression and activity in HFD-induced obese mice was tested. In 3T3-L1 adipocytes that overexpress PKD1 with altered activity, distribution of PKD1 within the cell was analyzed using immunofluorescent staining.

As second goal, this study elucidated the impact of PKD1 on lipolysis rate in adipocytes. To test a dependency, lipolysis essay was conducted with murine adipose tissue specifically deficient for PKD1.

Finally, aim of this study was also to test the effect of PKD1 deletion in adipocytes on the expression of genes implicated in regulation of energy dissipation in adipocytes.

Hereby a better understanding of the role of PKD1 in the regulation of adipose tissue function, especially in energy dissipation, and dysfunction of adipocytes in the context of obesity should be given.

2 Materials

2.1 Cell line

All experiments on cells from the cell culture were performed with 3T3-L1 mouse embryonic fibroblasts (ATCC® CL-173™) obtained from the American Type Culture Collection. Cells were grown and differentiated into adipocytes as described in 3.1.

2.2 Mouse models

Epigonadal white adipose tissue (epiWAT) from male C57BL/6 mice was kindly provided by the research group G. Sumara at Rudolf-Virchow-Zentrum Würzburg.

PKD1$^{flox/flox}$ mice [54] and adiponectin promotor-driven Cre mice [69] were purchased from Jackson Laboratory. From these, AG Sumara generated PKD1-knockout (PKD1$^{adipo.\Delta/\Delta}$) mice with specific deletion of PKD1 in white and brown adipose tissue. The region between the loxP sites is deleted by Cre recombinase in adipocytes [54].

Animal experiments were approved by the local institutional animal care (Regierung von Unterfranken, Germany) and conform to regulations of state. Animal protocol number AK 55.2-2531.01-124/13, approved on 28.01.2014.

2.3 siRNA and accessories

To knock down PKD1 and ATGL in adipocytes from cell culture small interfering RNA (siRNA) was used. With the method called RNA interference (RNAi) siRNA has the ability to cleave complementary mRNA targets and therefore silence its protein [70].
All products were purchased from Dharmacon™ GE Healthcare and prepared as recommended in protocols provided by the company. One volume of Dharmacon 5x siRNA Buffer (Cat.-No.: B-002000-UB-100) was diluted in four volumes of RNAse-free water (Cat.-No.: B-002000-WB-100) to generate a 1x solution in which siRNA was resuspended to a 20 µM stock. To ensure quality for every use, the suspension was aliquoted and stored at -20 °C [71]. For transfection DharmaFECT Duo Transfection Reagent (Cat.-No.: T-2010-03) was used as described in 3.1.3.

Description	Catalogue No.:	Target sequence
siGENOME Mouse	M-048415-01-0005	
SMARTpool siRNA, Prkd1	D-048415-01	GAAGAGAUGUAGCUAUUAA
	D-048415-02	GAAAGAGUGUUUGUUGUUA
	D-048415-03	CAUAAGAGAUGUGCAUUUA
	D-048415-04	CAGCGAAUGUAGUGUAUUA
siGENOME Mouse	M-040220-01-0020	
SMARTpool siRNA, Pnpla2	D-040220-01	GAAAUUGGGUGACCAUCUG
(Synonym: ATGL)	D-040220-02	GGAGAGAACGUCAUCAUAU
	D-040220-03	GCACAUUUAUCCCGGUGUA
	D-040220-04	UGAAGCAGGUGCCAACAUU
siGENOME Non-Targeting siRNA #1	D-001210-01-20	UAGCGACUAAACACAUCAA

2.4 Plasmids and accessoires

Electroporation technique with 4D-Nucleofector™ X Unit was used to introduce plasmids to cells. For both, 3T3-L1 pre-adipocytes and fully differentiated adipocytes SE Cell Line 4D-Nucleofector® X Kit L (24 RCT) was purchased from Lonza.

All Flag-tagged PKD1 plasmids including wild type (wt), kinase dead (kd), and constitutive active (ca) forms as well as the non-expressing empty vector were kindly provided by Romeo Ricci (Institute of Cell Biology, ETH Zurich, Switzerland) and stored at our laboratory of G. Sumara research group. Constitutively active kinase is generated by mutation of murine PKD1 at ser-744 and ser-748 sites to glutamic acid mimicking phosphorylation, whereas alteration to alanine of these sited results in a kinase that is resistant to phosphorylation and therefore cannot be activated [32].

Expression	Name of plasmid
empty	pcDNA5 Flag-empty

PKD1, wild type	pcDNA5 Flag-PKD1 WT
PKD1, kinase dead	pcDNA5 Flag-PKD1 KD
PKD1, constitutive active	pcDNA5 Flag-PKD1 2S2E

2.5 Antibodies

Primary antibodies were stored at -20 °C and freshly diluted for use as recommended in TBST with 5 % BSA. Dilutions were frozen and repetitively used.

Primary antibody target	Specification & Product No.	Supplier
GAPDH	Rabbit; G9545	Sigma-Aldrich
β-Actin	Mouse, monoclonal; A5441	Sigma-Aldrich
ATGL	Rabbit mAb; #2439	Cell Signaling
PKD/PKCμ	Rabbit; #2052	Cell Signaling
Phospho-PKD/PKCμ Ser916	Rabbit; #2051	Cell Signaling
Phospho-PKD/PKCμ Ser744/748	Rabbit; #2054	Cell Signaling
DYKDDDDK Tag (9A3) (Synonym: Anti-Flag® M2 trademark by Sigma-Aldrich)	Mouse mAb; #8146	Cell Signaling

Both secondary antibodies were kept at 4 °C. For use in Western blot, they were diluted in TBST-milk with 5 % BSA.

Secondary antibody	Specification & Product No.	Supplier
Anti-Rabbit	Goat; AMDEX; IgG Horseradish Peroxidase Conjugate GERPN4301	Sigma-Aldrich
Anti-Mouse	Sheep; AMDEX; IgG-HRP GERPN4201	Sigma-Aldrich

Secondary antibodies used for immunofluorescence were protected from light.

Secondary antibody	Specification & Product No.	Supplier

Anti-Goat	Donkey; polyclonal; IgG Alexa fluor® 568 conjugate	Thermo Fisher Scientific, life technologies
Anti-mouse	Mouse; IgG (H+L); polyclonal, Alexa fluor® 488 conjugate A-11001	Thermo Fisher Scientific, life technologies

Fluoroshield™ with DAPI, histology mounting medium from Sigma-Aldrich, was used for fluorescence preservation and DNA counterstaining.

2.6 Primer

Primer specificity was investigated using Primer-BLAST program provided by NCBI and ordered from Eurofins Genomics. The manufacturer provided dilution instructions for 100 µM dilutions. After dilution, primer were stored at -20 °C and for direct use in qRT-PCR diluted to 10 µM with RNase-free water.

RPL13a was chosen to be a suitable housekeeping gene for relative gene expression analysis [72].

Name of gene	Primer sequence (5' → 3')	Accession number
Protein kinase D 1, exon 1-2		NM_008858.3
- foreward primer	GGGGGCATCTCGTTCCATC	
- reverse primer	GTGCCGAAAAAGCAGGATCTT	
Protein kinase D 1, pair 3		NM_008858.3
- foreward primer	CCGTGAGAAGAGGTCAAATTCG	
- reverse primer	GTGGCACCTTCACCTTAGACA	
Ribosomal protein L13a		NM_009438
- foreward primer	CCCTCCACCCTATGACAAGA	
- reverse primer	GCCCCAGGTAAGCAAACTT	
Patatin-like phospholipase domain containing 2 (Pnpla2; Synonym: ATGL)		NM_025802

- foreward primer CAACGCCACTCACATCTACGG
- reverse primer GGACACCTCAATAATGTTGGCAC

2.7 Chemicals and reagents

Chemicals

Chemical	Supplier
Ethanol 96%	Carl Roth
Chloroform ≥ 99%	Carl Roth
Methanol, BioChemica	PanReac AppliChem
Albumin fraction V, ≥ 98 %, pulverized	Carl Roth
Bovine serum albumin, fatty acid free, ≥ 96 %, pulverized	Sigma-Aldrich
TEMED 99 %	Carl Roth
Glycin	Carl Roth
TRIS, PUFFERAN ≥ 99,3 %	Carl Roth
Glycine ≥ 99 %	Carl Roth
Powdered milk	Carl Roth
Protease and phosphatase inhibitor cocktail (100X)	Thermo Scientific
Triton® X 100	Carl Roth
Nonidet™ P 40 substitute (NP40)	Sigma Aldrich
Sodium chloride ≥ 99 % (NaCl)	Carl Roth
Hydrochloric acid (HCl)	Sigma Aldrich
Tween® 20	Carl Roth
SDS Pellets ≥ 99 %, for biochemestry	Carl Roth
Ammonium peroxydisulphate (APS) ≥98 %, p.a., ACS	Carl Roth

Acrylamide	
Adenosine 5'-triphosphate disodium salt hydrate, grade I, ≥99 %, from microbial	Sigma Aldrich
(−)-Isoproterenol (+)-bitartrate salt, powder (I2760)	Sigma Aldrich
Paraformaldehyde, extra pure, DAC	Carl Roth

Reagents

Free Glycerol Reagent	Sigma-Aldrich
NEFA-HR (2)	Wako
Clarity Western ECL Substrate	BioRad
Restore Plus Western Blot Stripping Buffer	Thermo Scientific
QIAzol lysis Reagent	QIAGEN
Bradford Protein Assay, Quick Start	BioRad
SYBR Green Master (ROX), FastStart Universal	Roche
PageRuler Plus Prestained Protein Ladder	Thermo Scientific
First Strand cDNA Synthesis Kit	Thermo Scientific

2.8 Buffer and other recipes

All self-made buffers were made freshly with ultra pure water (UPW).

Lysis buffer	384 ml 20 mM TRIS (pH 7.5)
	384 ml 150 mM NaCl
	384 ml 20 mM β-glycerophosphate
	1 ml 5 mM MgCl
	5 ml 5 % glycerol
	200 µl 0.2 % NP40
	200 µl 0.2 % Triton X-100

	aliquots of 10 ml were stored at -20 °C and thawed before use
10 x Tris-buffered saline (10 x TBS)	24.2 g TRIS 80 g NaCl added up to 1 l solution with UPW and adjusted to pH 7.6 with HCl
TBS	100 ml 10 x TBS 900 ml UPW
1 x TBS 0.1 % Tween (TBST)	999 ml TBS 1 ml Tween
TBST 5 % milk (TBST-milk)	100 ml TBST 5 g powdered milk
10 x running buffer-stock	30.27 g TRIS 144.0 g glycine add up to 1 l total volume with UPW
1 x running buffer	100 ml 10 x running buffer-stock 900 ml UPW 5 ml 20% SDS
1 x transfer buffer (storage: 4 °C)	100 ml 10 x running buffer-stock 700 ml UPW 200 ml methanol
1.5 M TRIS-stock, pH 8.6	90.82 g TRIS 500 ml UPW adjusted to pH 8.6 with HCl
2 M TRIS-stock, pH 6.8	121.1 g TRIS 500 ml UPW adjusted to pH 6.8 with HCl
8 % separating gel	10.7 ml UPW 5 ml 1.5 M TRIS pH 8.6 384 ml 40 % acylamide

	100 µl 20 % SDS
	200 µl 10 % APS
	20 µl TEMED
10 % separating gel	9.8 ml UPW
	5 ml 1.5 M TRIS pH 8.6
	5 ml 40 % acylamide
	100 µl 20 % SDS
	67.6 µl 10 % APS
	17.5 µl TEMED
4 % stacking gel	8.2 ml UPW
	620 µl 2 M TRIS pH 8.6
	946 µl 40 % acylamide
	50 µl 20 % SDS
	100 µl 10 % APS
	10 µl TEMED
Loading dye (Lammelli buffer)	1.5 ml 300mM Tris pH 6.8 (2M stock)
	1g 10% SDS
	5mL 50% glycerol
	2.5mL 25% β-mecaptoethanol
	spatula tip Bromophenolblue

2.9 Media and cell culture solutions

Item	Catalogue number	Supplier
DMEM, high glucose, GlutaMAX™ Supplement, pyruvate	31966-021	Gibco® life technologies
DMEM, low glucose, pyruvate	31885-023	Gibco® life technologies
DPBS, no calcium, no magnesium	14190-094	Gibco® life technologies
Gentamicin (10 mg/mL)	15710-049	Gibco® life technologies
Insulin solution human	I9278	Sigma-Aldrich
Trypsin-EDTA (0.05%), phenol red	25300-054	Gibco® life technologies

FBS (Fetal Bovine Serum, qualified, E.U.-approved, South America origin)	10270-106	Gibco® life technologies
FCS (Calf bovine serum, iron fortified)	30-2030	ATCC®
Accutase® solution	A6964	Sigma-Aldrich
Tryptan blue stain (0.4%)	T10282	life-technologies
Dexamethasone		
IBMX		
BD Matrigel™ matrix growth factor reduced	356230	BD Biosciences
Opti-MEM® I reduced serum medium	31985-070	Gibco® life technologies

2.10 Consumables

Consumption Item	Supplier
Pipette tips (0.5 – 20, 2 – 200, 1000 µl)	Biosphere
Filter tips (0.5 – 20, 2 – 200, 1250 µl)	Biosphere
Repetitive pipette tips (0.1, 0.5, 1.25, 2.5, 5.0 ml)	VWR
Tubes (15, 50 ml)	Sarstedt
Tubes, SafeSeal (0.5, 1.5, 2.0 ml)	Sarstedt
Powder free nitrile examination gloves, S	Medline
Pasteur pipettes	Carl Roth
Super RX medical x-Ray	Fujifilm
Blotting and chromatography papers, grade 3 MM CHR, 46 x 57 cm	Whatman
Immobilon-P transfer membrane, PVDF 0.45 µm	EMD Millipore
384-Well clear optical reaction plate, ABI PRISM, Applied Biosystems	life-technologies
Optical adhesive film, MicroAmp, Applied Biosystems	life-technologies
Standard scissors	Fine Science Tools
Standard and fine foreceps	

Tissue culture dish 100 (Standard, Cell+)	Sarstedt
Tissue culture plate Cell+ (6-well, 12-well)	Sarstedt
Syringe filter, Filtropur S 0.2	Sarstedt
Serological pipette (5, 10, 25 ml)	Sarstedt
MicroAmp™ Optical 384-well clear optical reaction plate	Applied Biosystems
MicroAmp™ Optical adhesive film	Applied Biosystems
Cover slip, round, 18 mm	Carl Roth
Microscope slides, 76 x 26 mm	Carl Roth
Parafilm® M	Carl Roth

2.11 Instruments and equipment

Technical Device	Supplier
Autoclave sterilizer, Systec DX-100	Microbiology International
Autoclave, Systec VX-120	Microbiology International
Ultrapure water, TKA GenPure xCAD	Thermo Fischer Scientific
Digital scale, TE3102S	Sartorius
Digital scale, EL303	Mettler Toledo
Microplate analyzer, Victor³ 1420	PerkinElmer
Water bath, 20mT	P-D Industriegesellschaft mbH Prüfgerätewerk Dresden
Multifuge X3R	Heraeus
Centrifuge 5424 R	Eppendorf
Thermomixer comfort	Eppendorf
Microcentrifuge, Galaxy MiniStar	VWR
Vortexer, RS-VA 10	Phoenix Instrument
Magnetic stirrer, RSM-10HP	Phoenix Instrument
Incubator, Hera Cell 240	Heraeus
Incubator, C150	Binder
Vertical flow hood	BDK Luft- und Reinraumtechnik

	GmbH
Microscope, CKX31	Olympus
Counting champers	Neubauer-improved
Sequence detection system, ABI Prism 7900HT, Applied Biosystems	life-technologies
Thermal cycler, T100	BioRad
Electronic repeat pipettor, Repetman	Gilson
Pipetts (different sizes)	Eppendorf, VWR
Motorized pipette controller	Gilson
x-ray cassette	Amersham Biosciences
Bench-top homogenizer, PT 1600E	Polytron
pH-meter, FiveEasy FE20	Mettler Toledo
Power supply, EPS-300X	C.B.S. Scientific
X-ray film processor, Cawomat 2000 IR	CAWO
Spectrophotometer, NanoDrop 2000 c	Thermo Scientific
4D-Nucleofector™ X Unit	Lonza
Automated upright mircoscope system, Leica DM5500 B	Leica Microsystems

2.12 Software

Following software was used to gather, process, and analyze data:

Wallac 1429 Workstation

Microsoft Office Word, Excell, Powerpoint 2011

AdobeReader

SDS 2.2 Software (qRT-PCR) Applied Biosystems

Leica Application Suite (LAS) AF lite provided by Leica Microsystems

Adobe Illustrator CC

3 Methods

3.1 Cell culture

3T3-L1 cells were cultured using protocol provided by ATCC briefly summarized as follows. Standard incubation procedures were performed at 37 °C, 95% humidity and a 5% CO_2 concentration maintained by a suitable incubator. Medium was always heated to 37 °C before use except when stated differently. FCS and FBS were inactivated in water bath at 56 °C for 30 minutes and aliquoted in 50 ml tubes to be stored at -20 °C. Before use, proper amounts were thawed and heated to 37 °C again. All work with cells was done using the aseptic bench top and spraying utilities with 70 % ethanol to guarantee aseptic conditions.

For long-term storage 3T3-L1 pre-adipocytes were maintained in DMEM high glucose media containing 10% FCS and 5% DMSO in cryopreservation tubes and kept in -80 °C for 24 hours before placed in liquid nitrogen until ready for use as described in ATCC 3T3-L1 product sheet.

3T3-L1 cells were grown in growth medium composed of DMEM high glucose, 10 % FCS, and 0.4 % gentamicine in 100 mm tissue culture dishes with a total of 10 ml growth medium per dish in an incubator for proliferation. Growth medium was exchanged every 2 – 3 days to obtain appropriate concentrations as recommended by ATCC. If sub-culturing of cells was intended, cells were not allowed to reach more than approximately 70 % confluence [73]. In this case, growth medium was removed and cells on the dish were gently washed with PBS. 2.0 ml Trypsin was added onto each dish and kept in the incubator for approximately 2 minutes until cells could detach. The new passage of cells was collected, spun down, and resuspended in growth media to be split onto tissue culture dishes again. For experiments, passage numbers no higher than 11 were used.

3.1.1 3T3-L1 adipocyte differentiation

In order to induce differentiation of 3T3-L1 pre-adipocytes into adipocytes as recommended by ATCC, cells were grown to confluence and maintained post-

confluent for 48 hours [73]. Then, growth medium was replaced with differentiation medium composed of DMEM high glucose, 10 % FBS, 0.4 % gentamicine, 1.0 µM dexamethasone, 0.5 mM IBMX, and 1.0 µg/ml Insulin. After 48 hours of incubation the medium again was replaced by maintenance medium containing only DMEM high glucose, 10 % FBS, 0.4 % gentamicine, and 1.0 µg/ml insulin. Medium was renewed every 2 – 3 days and cells were fully differentiated after 7-13 days.

3.1.2 Replating 3T3-L1 adipocytes for conduction of experiments

When experiments with differentiated 3T3-L1 adipocytes were to be performed, they were collected and re-plated in the following manner: Depending on the experiment, either 6- or 12-well plates were prepared with 250 or 500 µl of ice-cold PBS with 0.5 % matrigel per well. After 30 minutes in the incubator the solution was gently removed and washed off with ice-cold PBS again. This preparation supports reattachment of adipocytes and prevents detachment concurrently, since mature adipocytes rather float on the surface of liquids. Meanwhile, media was removed from the adipocytes in the 100 mm dish and 4 ml of accutase solution was spread on each dish. After 10 minutes of incubation adipocytes started to detach, were washed off the dish with the maintenance media, and pipetted in a 50 ml tube. The tube containing the adipocytes was then centrifuged at 125 x g for 5 minutes. The supernatant was removed and remaining cell pellet was dissolved in regular maintenance media for counting and proper distribution into the prepared 6- or 12-well dish at a certain cell density as described in the experiments.

3.1.3 Transfection of cells using siRNA

Transfection was performed when 3T3-L1 adipocytes reached state of full differentiation as described in 3.1. Either 6- or 12-well plates had to be prepared beforehand as stated in 3.1 depending on the purpose of the experiment: 6-well plates were used for Western blot analysis of proteins and for quantitative PCR to detect RNA levels 12-well plates were used.

After harvest of cells as described in 3.1 they initally were not seeded but kept in a 50 ml tube diluted in maintenance media to be counted using Neubauer cell counting

chamber. For counting, 50 µl of carefully mixed cell solution was stained with 50 µl of tryptan blue. Only living cells that appeared bright, were counted in 4 squares (4 mm^2), then devided by 4 to provide the average. This number of cells was multiplied by the dilution factor with tryptan blue (2) and the factor of Neubauer counting chamber (10,000) which gives the total amount of cells per milliliter [74].

For efficient siRNA transfection of 3T3-L1 adipocytes 1.16 x 10^5 cells/cm^2 were used following instructions for optimization of transfection recommended by Kilroy et al. [75]. The number of recommended cells per cm^2 equals 4.64 x 10^5 adipocytes per well in a 12-well plate (approximately 4 cm^2 per well) and 11.136 x 10^5 adipocytes per well in a 6-well plate (approximately 9.6 cm^2 per well). The appropriate amount of 1 µl 20 mM siRNA/cm^2 was mixed with 10 µl OptiMEM/cm^2 and left in a tube at room temperature for 5 minutes. Then 1.4 µl DharmaFECT Duo/cm^2 combined with 18.6 µl optiMEM/cm^2 were added to the first tube. After 20 minutes the equivalent amount of cells per cm^2 was added to the tube whereupon the complete solution was spread on either a 6- or a 12-well plate according to the given parameter.
The maintenance medium needed to be changed every 24 hours.

3.1.4 Transfection of cells with plasmids

3T3-L1 pre-adipocytes and fully differentiated adipocytes (3.1) were transfected with plasmids via electroporation using Lonza's 4D-Nucleofector™ technology. The cell-specific protocol and program were provided by Lonza. According to the manufacturer, the program CM-137 was used to transfect 3T3-L1 pre-adipocytes and CM-133 for adipocytes [76]. Minor changes were undertaken when plating transfected cells for immunofluorescent staining: One 100 µl cuvette was spread on 4 wells of a 12-well plate containing cover slips prepared with 0.5 % matrigel coating as stated before (3.1). This approach guaranteed well-distributed and less overlaying cells on slides allowing better examination under the microscope. Transfected cells were kept in culture for 24 hours until further analyzed.
Transfection efficiency was confirmed using GFP-vector transfected cells provided in Lonza's kit.

3.1.5 Immunofluorescence

For immunofluorescent staining, cells were plated on cover slips in 12-well plates (3.1.4). The cells were washed with PBS 3 times before fixation with 4 % paraformaldehyde in PBS at room temperature for 10 minutes [77]. After washing 3 times with PBS the cells were permeabilized with 0.1 % triton X-100 in PBS for 15 minutes at room temperature. Cells were blocked with 2 % BSA in PBS for 1 hour until repeatedly washed and ready for antibody incubation. To save supplies of antibody incubation process, cover slips were transferred on parafilm placed inside a wet chamber.

Primary anti-flag® antibody was diluted 1:1600 in PBS containing 1 % BSA and approximately 100 µl was distributed onto each cover slip except the negative control containing secondary antibody only. After an over-night incubation at 4 °C cover slips were washed 3 times with PBS and incubated with anti-goat alexa fluor® 568 conjugate secondary antibody (1:500 in PBS 0.5 % BSA, 90 minutes, 4°C) except negative control containing primary antibody only. Again, cover slips were washed 3 times with PBS. Then, they were covered with phalloidin-iFluor 555 reagent according to the manufacturers (abcam) instructions in PBS 1 % BSA for 90 minutes. Thereafter, they were washed 3 times with PBS again. Approximately 50 µl mounting medium containing DAPI was used to fixate cover slips on the glass-slides and co-stain the nucleus. Finished slides were then kept in the dark at 4 °C. Analysis under the microscope was possible one day after mounting. The primary and secondary negative controls used for validation of the efficiency of method did not display fluorescent activity (data not shown).

Pictures were taken with 63X-objective of mircoscope system from Leica.

3.2 Mouse adipose tissue under different metabolic conditions

Mouse adipose tissue samples for the fasting experiment (4.1.1) were taken from mice that had free access to normal rodents chow diet (ND). The experiment was conducted with nine mice for the 12-hour and nine mice for the 24-hour fasting experiment. Six of each were withdrawn from food for either 12 hours over night or for 24 hours. Of these, three mice were refed in each experimental group after 12 or 24 hours again.

For experimental comparison of PKD1 response to normal and high fat diet (4.2), 8 mice were fed with ND supplied by the institutes animal house and 7 mice with high caloric rodents diet (HFD) containing 58 kcal% fat and sucrose (Product-No.: D12331 from Research Diets) for 24 weeks.

PKD1$_{flox/flox}$-mice and PKD1$_{adipo.\Delta/\Delta}$-mice were either on ND (4.4) or fed with HFD for 24 weeks (4.5) before conducting the analysis.

3.2.1 Dissection of adipose tissue

After mice were sacrificed via cervical dislocation, epigonadal white adipose tissue (epiWAT) was quickly taken from the abdomen, subcutaneous white adipose tissue (subWAT) from abdominal skin, and brown adipose tissue (BAT) from interscapular depot [1]. The tissue samples was then portioned in 2 ml tubes and flash frozen in liquid nitrogen for long time storage.

3.2.2 Mouse adipose tissue explants

For direct experiments on explants as in the isoproterenol stimulation experiments (4.1.2, 4.4) epiWAT were not frozen but directly kept in high glucose DMEM supplemented with 0.5% BSA and sectioned into 20 – 24 mg pieces. Until immediate beginning of experiment explants were incubated at 37 °C, 95% humidity and a 5% CO_2 concentration to ensure equal starting conditions.

3.3 Protein analysis

Analysis of protein levels of PKD1 and ATGL was conducted as follows:

After the medium had been removed, cells were collected by pipetting 150 µl lysis buffer containing 1 % PPI on each well and scratching cells off the plate with cell-scrapers. This step was done on ice to prevent degradation of the proteins during the process. The lysates were collected in tubes and stored at -80 °C.

When the explant adipose tissue was processed for protein analysis, 150 µl lysis buffer containing 1 % PPI was added, too. Explants were then homogenized in tubes with bench-top homogenizer at 15 Hz for 2 minutes.

The lysates (cells from cell culture as well as explant adipose tissue) were then placed on ice for 10 minutes whereupon they were centrifuged at 13000 rpm at 4 °C for 10 minutes. Centrifugation separated cell mass from a clear supernatant containing proteins, which was transferred to a new tube and stored at -80 °C.

The proteins were quantified using Quick Start Bradford Microplate Standard Protein Assay (0.05-0.5 mg/ml) as described in the manufacturers instruction manual. For the assay, protein samples were diluted 1:10 and after measurement, concentrations were calculated in excel by taking an average of duplicates. Thus, equal amounts of protein could be loaded to conduct Western blot.

Generally, quantities between 15 to 50 ug of protein were used depending on how well proteins of interest were detectable. The desired quantity of protein solution was pipetted into tubes. To balance the difference of volume to the most concentrated sample of one experiment, lysis buffer was added, so that all samples had the same concentration of protein. Each sample was mixed with 5 x loading dye and denaturated in a thermomixer at 95 °C for 5 minutes. The Proteins were separated by their molecular weight in sodium dodecylsulphate-polyacrylamide gel electrophoresis (SDS-PAGE) using 8 %- or 10 %-separating and 4 %-stacking gel. After building up the blotting system in running buffer, equal volumes of the prepared samples were loaded into pre-washed chambers. Electrophoresis was conducted at 100 to 130 V for 4 hours. The separated proteins were transferred onto a polyvinylidene difluoride (PVDF) membrane. Beforehand, PVDF membrane was activated in methanol. Then, the transfer box containing transfer buffer was build in the following order starting on the black side (anode) of the box: sponge, 4 sheets of filter paper, gel, PVDF membrane, 4 sheets of filter paper and sponge. At 75 mA the transfer of protein was completed over night. The PVDF membrane was blocked in TBST-milk for 1 hour at 4 °C, washed with TBST 3 times for 15 minutes at room temperature, and incubated with primary antibodies diluted in TBST 5 % BSA at 90 rpm as follows:

	Dilution	Incubation	kDa
PKD1	1:2000	4°C over night	115

PKD1 (Ser916)	1:1000	4°C over night	115
PKD1 (Ser744/748)	1:1000	4°C over night	115
ATGL	1:5000	4°C over night	54
PKD2	1:1000	4°C over night	105
PKD3	1:1000	4°C over night	110
Anti-beta-Actin	1:5000	1h room temp.	42
GAPDH	1:10.000	4°C over night	36
	1:5000	1h room temp.	

The membrane was washed 3 times with TBST again before it was incubated with secondary antibodies in TBST-milk targeting either rabbit (1:5000 dilution) or mouse antibodies (1:10000 dilution) in case of GAPDH for one hour. After washing with TBST and finally with TBS, protein detection was performed by covering the membrane with ECL substrate for 5 minutes. Then images were taken via exposure to X-ray film for 1 second up to 10 minutes depending of the strength of light emission. For comparison, actin and GAPDH were used to prove an equal loading of protein.

3.4 RNA analysis

For ribonucleic acid (RNA) level measurements, cells from culture were resuspended in 1 ml QIAzol per well, thoroughly scratched off the plate, collected in 2 ml tubes and rapidly frozen on dry ice. When analyzing RNA of epiWAT, subWAT, and BAT taken from mice (3.2.1), samples were homogenized with bench-top homogenizer at 15 Hz for 2 minutes in 2 ml tubes containing 1 ml QIAzol and flash frozen in liquid nitrogen. Samples could either be stored at -80 °C or processed directly. Before processing, frozen samples needed to defreeze on ice. In order to extract RNA, samples were processed acting on the suggestion of quick-start protocol provided by QIAGEN starting from step 3 [78].

RNA was quantified with NanoDrop 2000 c spectrophotometer. 2.0 µl RNAse free water was used as blank and concentration (in µg/ml) of nucleic acid was measured in

2.0 µl of each RNA solution with absorbance at 230nm, 260nm, and 280nm. To guarantee RNA purity, ratios of 260nm/230nm and 260nm/280nm were calculated. According to the manufacturers technical bulletin, absorbance at 230 nm is a result of contamination, e.g. traces of QIAzol. Hence, 260nm/230nm ratios of 2.0 – 2.2 as well as 260nm/280nm ratios of approximately 2.0 can be interpreted as pure RNA samples whereas lower 260nm/280nm ratios indicate contamination with protein or reagent [79].

Reverse transcription of RNA into complementary DNA (cDNA) was conducted with First Strand cDNA Synthesis Kit. Random hexamer primer provided by the kit were used to ensure that all RNA was transcribed. An oligo$(dT)_{18}$ primer binds only messenger RNA (mRNA) with poly(A) tail and was not used in this study. Following the protocol provided by the manufacturer, samples were pipetted in the following manner:

1 µg of total RNA

1 µl of random hexamer primer

RNase-free water added up to 11 µl

Then, samples were incubated at 65 °C for 5 minutes as recommended in the protocol and an enzyme mixture was added containing the following:

4µl 5X reaction buffer

1 µl RiboLock RNase Inhibitor

2 µl 10 mM dNTP Mix

2 µl M-MuLV Reverse Transcriptase

After vortexing and centrifugation, tubes were incubated at 25 °C for 5 minutes followed by 60 minutes at 37 °C and finally 5 minutes at 70 °C. For storage, prepared cDNA samples was stored at -20°C.

For further procedures, cDNA from explant tissues were diluted to 1:15 final concentration and cDNA from cultured cells to 1:3 with RNase-free water. 2 µl of the

cDNA samples (6.66 ng and 33.33 ng in total) were pipetted into a 384-well plate and mixed with 8 µl of the following master mix:

5 µl FastStart Universal SYBR Green Master (ROX)

0.4 µl of 10 µM forward primer (final concentration of 0.4 µM)

0.4 µl of 10 µM reverse primer (final concentration of 0.4 µM)

2.2 µl RNase-free water

FastStart Universal SYBR Green Master (ROX) from Roche is a ready-to-use master mix suitable for quantitative real-time polymerase chain reaction (qRT-PCR) as it contains all reagents necessary. With a fluorescent dye, double-stranded DNA can be detected. The DNA doubles at each amplification cycle and thus its quantity is proportional to the fluorescent signal. For relative quantification, threshold cycles (C_t) of samples were normalized to the C_t values of RPL13a as the housekeeping gene (primers are listed in 2.6). Data was then analyzed by comparison of the fold change in expression of specific genes in the samples [80]. First step of qRT-PCR is the activation of FastStart Taq DNA polymerase (contained in SYBR green) at 95°C for 10 minutes. Then, 40 cycles follow consisting one step denaturation of the double strand DNA (95°C for 15 seconds), annealing of the primers to the single stranded DNA, and elongation where DNA is synthesized using DNA polymerase (primer dependent temperature (2.6) for 60 seconds). Melting curve analysis was performed to exclude unspecific product amplification or primer-dimers [80].

Generally, RPL13a reached C_t values from 17 to 19. All other primers used had cycle numbers of 25 to 34.

3.5 Lipolysis essays

For investigation of lipolysis rate, samples of cells or explants were serum starved for 1 hour in a medium containing high glucose DMEM and 0.5 % FFA-free BSA. For control, sample were transferred to fresh starvation medium. For stimulation of lipolysis, samples were incubated in medium containing 10 µM isoproterenol for 2 hours.

FFAs in medium of the samples were quantified using NEFA-HR(2) reagent (Wako) according to manufacturers' instructions. Glycerol was measured with free glycerol reagent (Sigma-Aldrich) also as described by the manufacturer.

When samples of lipolysis experiments were tested for RNA levels with qRT-PCR, samples were incubated in medium containing 10 µM isoproterenol for 4 hours and then processed as described in 3.4.

3.6 Statistical analysis

Results and figures shown in this study were calculated with Microsoft Office Excel and drawn with Illustrator software. Results are presented as mean with ± standard error. To show differences between two groups Student's T-test was conducted and valuees of *$p < 0.05$ were considered as significant. Also **$p < 0.005$ and ***$p < 0.001$ were marked in the graphs.

4 Results

4.1 Regulation of PKD1 expression in adipocytes in response to different physiological conditions

Activity of adipocytes depends on the amount of nutrients available for the organism. Generally, upon excessive food ingestion adipocytes absorb the nutrients from circulation and convert them into TG [1]. In contrast, during food deprivation TG are degraded in the process of lipolysis to produce FFA and glycerol [14]. G. Sumaras research group showed that inactivation of PKD1 specifically in adipocytes results in pronounced effect on function of these cells (1.2.2).

4.1.1 Adipose tissue specific expression of PKD1 in response to fasting and feeding

To investigate regulation of PKD1 activity and PKD1 expression or abundance during feeding-fasting-cycles, Western Blot and RT-qPCR were used in the first experiment.

In a preliminary experiment conducted by M. Löffler, epigonadal white adipose tissue (epiWAT) was isolated from mice fed ad libidum, prolonged (24 hours, h) fasted animals, and mice, which were fasted for 24 h and re-fed for the same period of time. To test effect of fasting and feeding within a shorter time period, in an independent experiment of this study, one group of mice were subjected to fasting for 12h, other group was 12h-fasted followed by 12h re-feeding and compared to mice that had free access to food (ad libidum).

This experiment showed that 12 and 24 h fasting of mice results in reduction of PKD1 activity in epiWAT as assessed by Western Blot using antibody against PKD1 phosphorylated on serine 916 (Figure 4, A and B). Interestingly, re-feeding of mice brought phosphorylation of PKD1 on serine 916 to the levels observed in adipose tissue of unfastened animals (Figure 4, A and B, PKD1ser916). Reduced levels of phosphorylated PKD1 might be caused by diminished upstream mechanism phosphorylating this kinase or by lower total levels of PKD1 protein. To understand which of these two mechanisms regulate PKD1 activity in response to fasting, an antibody detecting total levels of PKD1 was used. Results of Western Blot suggest that total PKD1 protein levels are reduced in adipose tissue of fasted mice and that PKD1 is re-expressed upon re-feeding (Figure 4, A and B, PKD1).

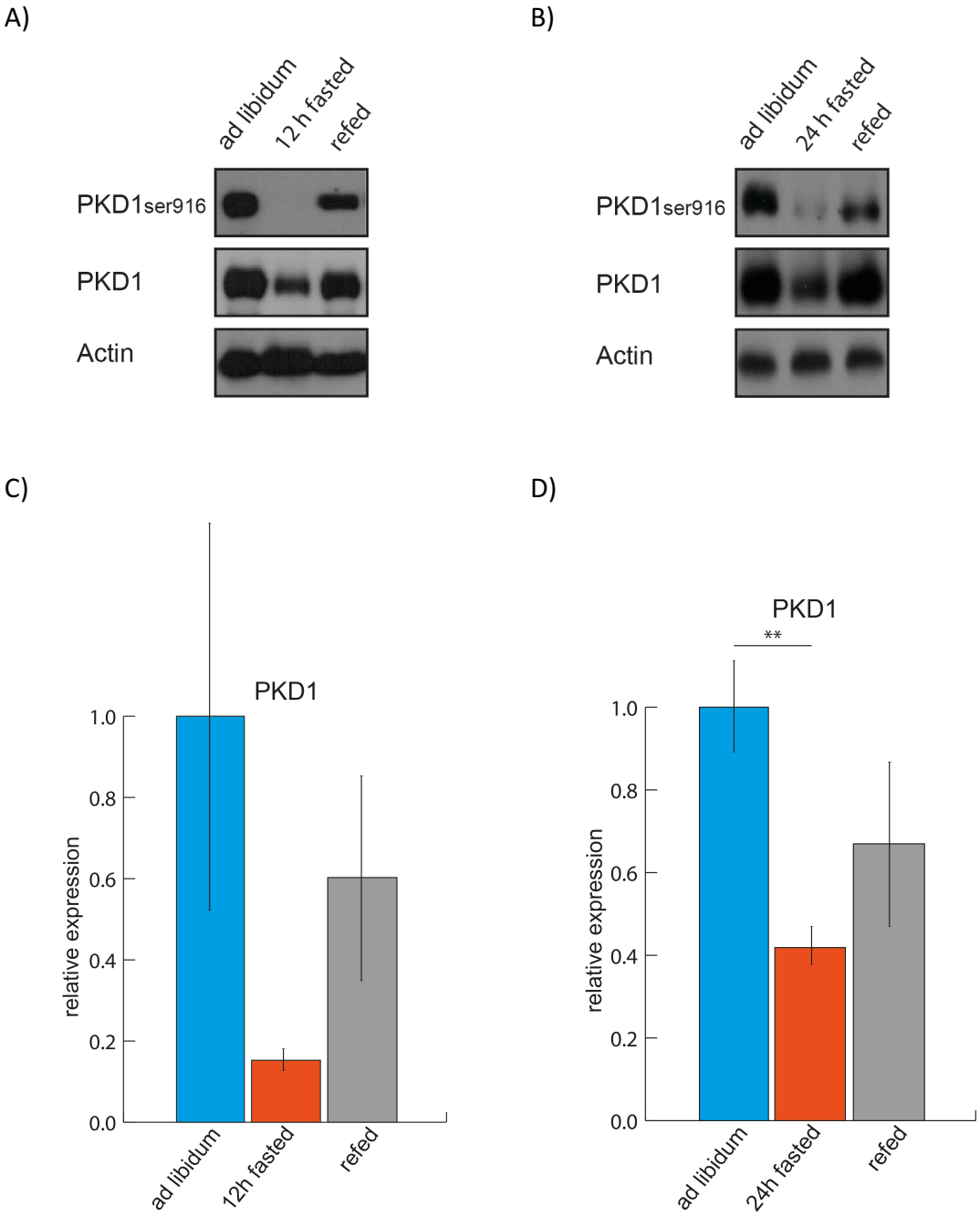

Figure 4: PKD1 protein levels, activity and gene expression in adipose tissue of mice are reduced upon fasting. For each experiment 9 mice had free access to normal chow diet (ad libidum) of which 6 mice were fasted for 12 hours overnight (A, C) and other 6 for 24 hours starting at night (B, D; conducted by M. Löffler). Afterwards 3 of the 6 fasted mice were exposed to food again for either 12 or 24 hours (refed). EpiWAT was examined in Western blot (A, B) and in RT-qPCR (C, D).

Therefore, reduction of phosphorylated PKD1 levels in fasted mice might be caused by lower RNA levels encoding this protein. In fact, RT-qPCR results indicate that RNA

levels encoding PKD1 are reduced upon both 12 and 24h fasting and expression is back to normal upon re-feeding of the animals (Figure 4, C and D).

In conclusion, it was shown that fasting reduces PKD1 transcription, which results in diminished PKD1 protein levels and activity.

4.1.2 Expression of PKD1 in adipocytes upon lipolytic stimuli

The expression of PKD1 diminished when mice were exposed to fasting (4.1.1). Upon fasting, TGs stored in adipocytes are hydrolyzed in the process of lipolysis [14]. Activation of β-adrenergic receptors is known to stimulate lipolysis in adipocytes [15, 20].

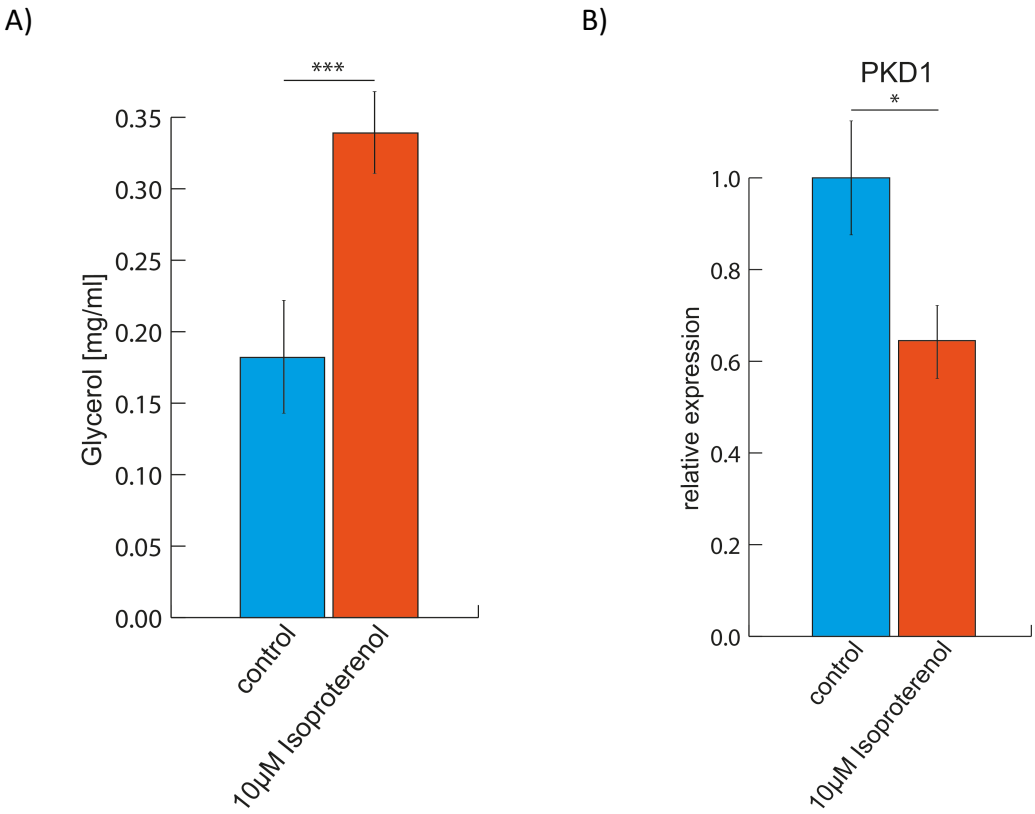

Figure 5: Increased lipolysis and decreased PKD1 expression in mouse epiWAT upon isoproterenol stimulation. EpiWAT was taken from one mouse and dissected. After 1 hour of starvation in a medium containing high glucose DMEM and 0.5 % FFA-free BSA explants were either transferred to starvation medium again (control; n=15) or in medium containing 10 µM isoproterenol (n=17). Glycerol levels in medium were measured after 2 hours of incubation (A) and RT-qPCR was conducted from explants after 4 hours (B).

Accordant with that, here isoproterenol as a potent stimulator that induces lipolysis in murine adipose tissue was confirmed: Glycerol levels were significantly elevated compared to no stimulation (Figure 5, A). It is of notice that isoproterenol is an agonist of β-adrenergic receptor, a GPCR, and induces cardiomyocyte hypertrophy in mice through the actions of PKD1 [54]. Therefore, the effect of isoproterenol-inducted lipolysis on PKD1 expression in adipocytes was tested. For this purpose, isolated adipose tissue explants were used. Interestingly, PKD1 expression was decreased when explant adipose tissue from regular black six mice were stimulated with isoproterenol (Figure 5, B), suggesting that induction of lipolysis might be required for suppression of PKD1 expression. This statistically significant reduction corresponds with the findings in adipose tissue of fasted mice (Figure 4, C and D).

However, adipose tissue is heterogeneous and also contains blood vessels, nerves, macrophages, and many other cell types [1]. To focus on one cell type only, isoproterenol experiment was conducted in vitro with differentiated 3T3-L1 adipocyte cell line and expression of PKD1 was measured.

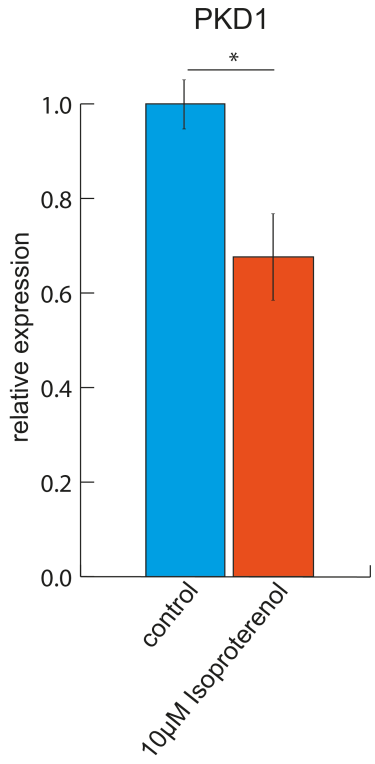

Figure 6: 3T3-L1 adipocytes show decreased PKD1 expression upon isoproterenol stimulation. Cells were incubated in starvation medium for 1 hour. Then medium was exchanged either to starvation

medium again (control; n=4) or to medium containing 10 µM isoproterenol (n=4). After 4 hours cells were collected and PKD1 expression was measured via RT-qPCR.

Again, isoproterenol treatment resulted in significantly reduced PKD1 RNA levels (Figure 6). These results demonstrate that isoproterenol not only induces lipolysis but also diminishes PKD1 expression in adipocytes ex vivo and in vitro.

4.1.3 Silencing of ATGL in adipocytes does not affect PKD1 expression

Next, it was analyzed whether enhanced lipolysis and its products can directly be associated with the decrease of PKD1 expression in adipocytes (4.1.2) or whether isoproterenol is responsible for this effect independently from lipolysis. Therefore, 3T3-L1 adipocytes were transfected with siRNA targeting adipose triglyceride lipase (ATGL), which initiates the three steps of triglyceride (TG) lipolysis [15]. It was shown before that ATGL knockout reduces FFA release (TG hydrolysis) up to 72 percent [16].

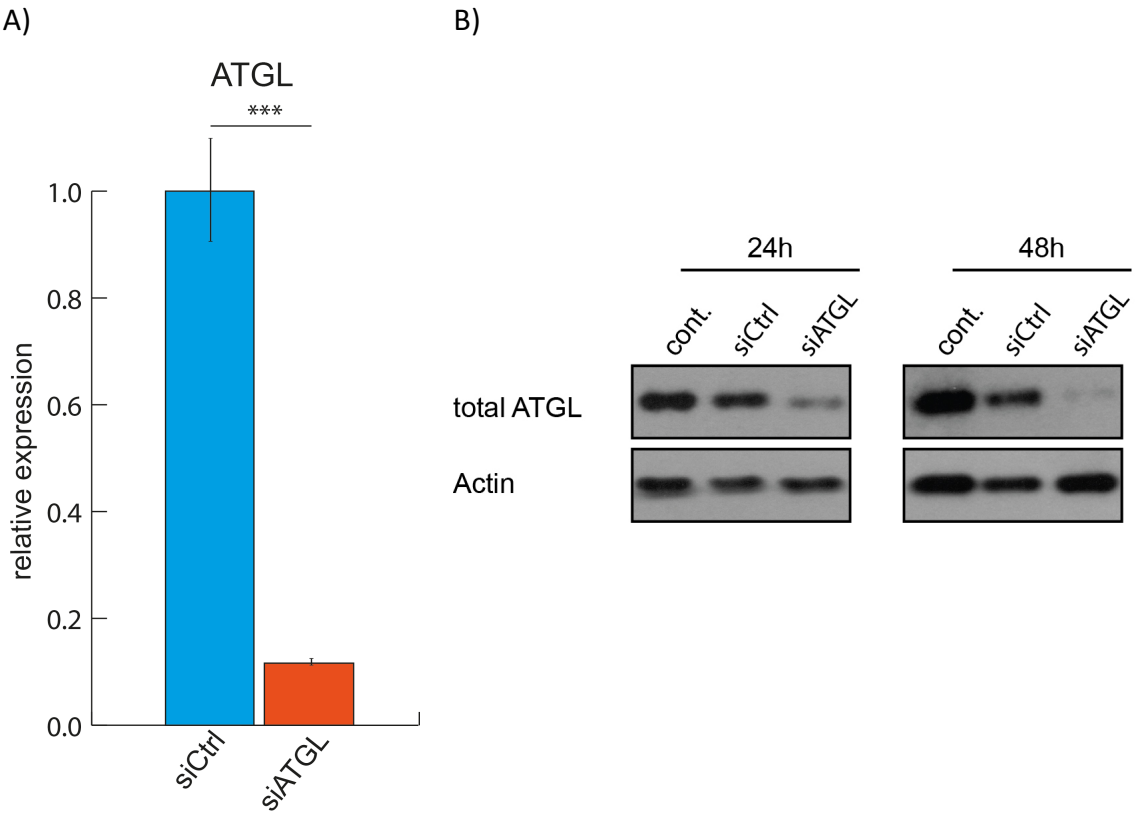

Figure 7: Silencing of ATGL in 3T3-L1 adipocytes after transfection with siRNA. Mature cells were transfected with siRNA targeting ATGL (adipose triglyceride lipase; siATGL; n=3) or non-targeting siRNA

(siCtrl, n=3) as a control and incubated for 24 hours. Controls (cont.) are non-treated 3T3-L1 adipocytes. Then cells were collected for RT-qPCR (A) and Western blot (B) analysis or medium was changed to maintenance medium and cells were collected after 48 hours for Western blot (B).

Silencing of ATGL was significantly sufficient on RNA and Protein level after 24 hours of transfection (Figure 7). Also, when comparing ATGL protein levels of non-treated cells (cont.) to adipocytes transfected with non-targeting siRNA (siCtrl) one can see that transfection only minimally affects physiological ATGL expression after 24 hours (Figure 7, B, 24 hours). However, when treated with siCtrl for 48 hours, little reduction of physiological ATGL protein levels were observed (Figure 7, B, 48 hours). Thus, further experiments with transfection were conducted after 24 hours and results were always compared to siCtrl-transfected cells.

Next, lipolysis essay was performed with transfected adipocytes at basal as well as isoproterenol-stimulated status. The basal TG lipolysis in 3T3-L1 adipocytes is not altered between siATGL- and siCtrl-transfected cells (Figure 8, A and B, control). But when stimulated with isoproterenol to enhance lipolysis, glycerol and FFA levels of siATGL-adipocytes remain low while values of siCrtl-treated adipocytes significantly increase. It is striking that cells transfected with siATGL have significantly diminished glycerol and FFA levels upon isoproterenol stimulation compared to siCtrl-cells (Figure 8, A and B). This is in line with findings of Scheiger et al. [16] suggesting that ATGL silencing effectively inhibits production of lipolytic products when stimulated with isoproterenol.

Analysis of transcriptional levels showed that ATGL silencing does not significantly affect PKD1 expression in 3T3-L1 adipocytes (Figure 8, C, control). Upon isoproterenol stimulation, PKD1 expression is down regulated in both control and ATGL-silenced adipocytes. Altogether, these results might indicate that isoproterenol independently from TG lipolysis lowers PKD1 expression in 3T3-L1 adipocytes and inhibition of lipolysis through ATGL-silencing has no significant effect on PKD1 on RNA level.

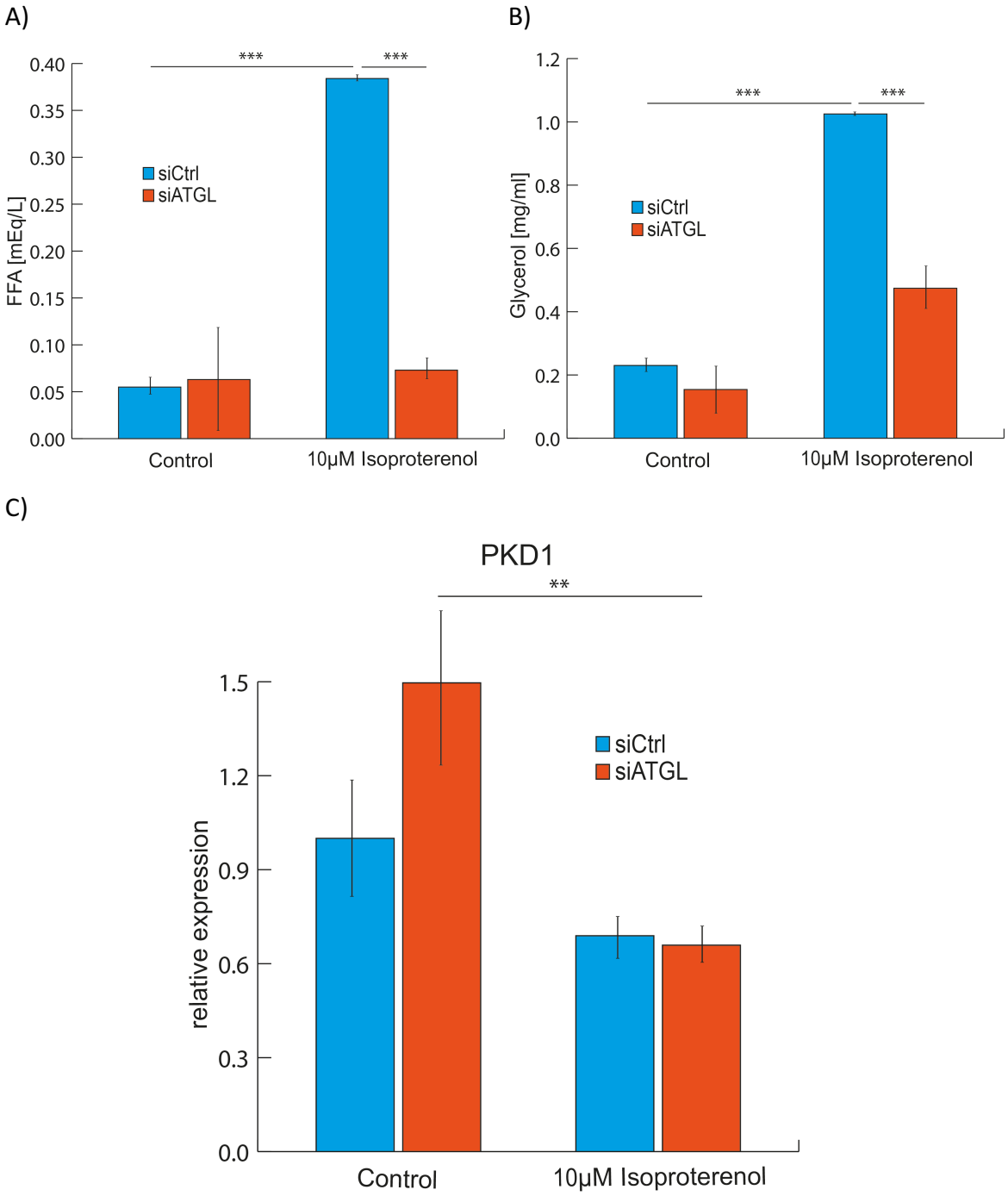

Figure 8: ATGL silencing does not affect PKD1 expression in 3T3-L1 adipocytes. 3T3-L1 adipocytes were transfected with non-targeting (siCtrl) and ATGL-targeting (siATGL) siRNA for 24 hours. Then they were exposed to starvation medium for 2 hours and either starvation medium was changed (Control, n=4/siRNA type) or medium with 10 µM isoproterenol was added (n=4/siRNA type). After 2 hours FFA- and glycerol-levels were analyzed (A, B). Relative PKD1 expression was measured after 4 hours incubation (C).

4.2 PKD1 expression is altered in adipose tissue of obese mice

PKD1 was identified as a novel gene locus that is associated with BMI [68]. Previous studies by G. Sumara research group were performed to address the function of PKD1 in lipid accumulation in adipose tissue in vivo (1.2.2). To assess the role of PKD1 during stages of over-nutrition mouse adipose tissue, mice were fed with HFD (58 kcal% fat and sucrose) for 24 weeks until obesity was induced in these mice (Figure 3, A, PKD1$^{flox/flox}$ HFD).

Here, adipose tissue of mice at the condition of over-nutrition described above were compared with adipose tissue of littermates fed with ND and effect on PKD1 expression in white adipose tissue was analyzed by RT-qPCR.

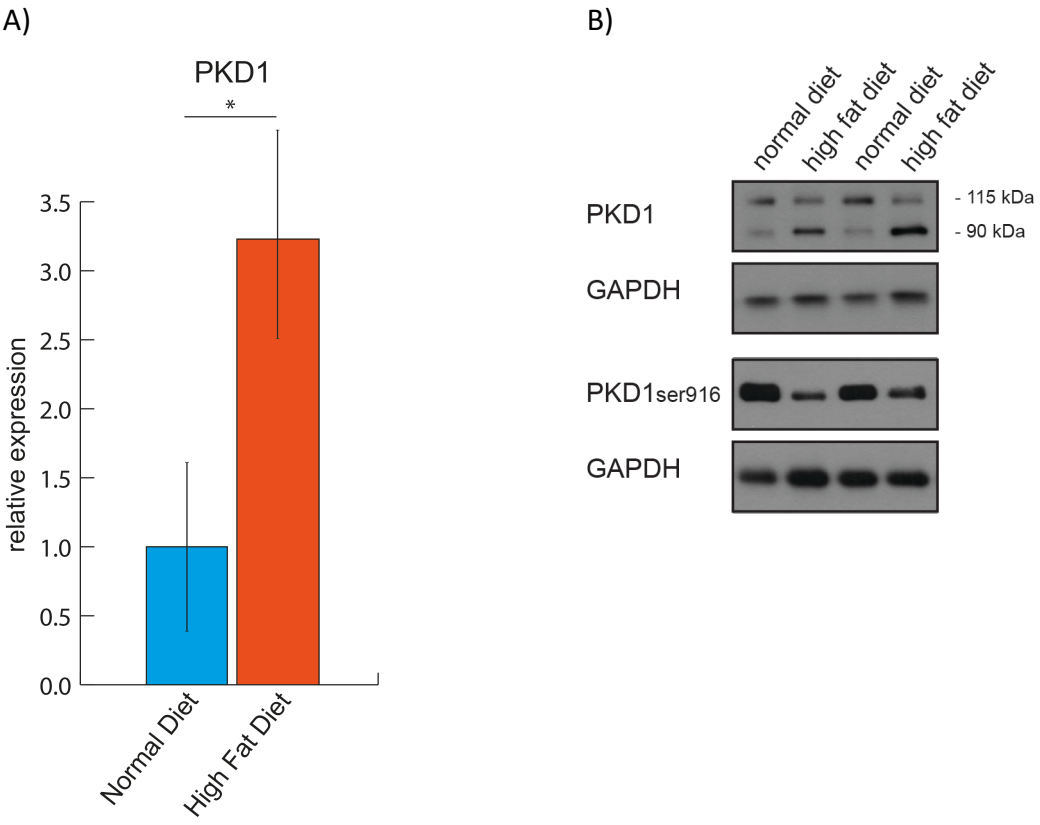

Figure 9: EpiWAT from mice fed HFD display increased PKD1 expression in comparison to ND. Mice of the same litter were fed high caloric diet (HFD; n=7) containing 58 kcal% fat and sucrose or normal chow diet (normal diet; n=7) for 24 weeks. RT-qPCR (A) and Western blot (B) were performed with epiWAT of these mice.

In fact, RNA analysis shows that PKD1 expression is significantly elevated in response to high caloric life-style of mice (HFD), compared with epiWAT of mice on ND (Figure 9, A). Hence, results of RT-qPCR indicate that PKD1 levels increase during lipogenesis and possibly during adipocyte hypertrophy.

Also, translation of PKD1 on protein level in these two groups was analyzed (Figure 9, B). Although PKD1 RNA levels indicate differently, here total PKD1 clearly appears to be up regulated upon ND and down regulated upon HFD. Consistent with the pattern of the Western blot, level of the phosphorylated form PKD1 ser-916, which represents the activated form of PKD1, appears to be higher in mice fed with ND than mice on HFD, too. These results stand in contrast to the findings in RT-qPCR. Interestingly, a second lower band appears at approximately 90 kDa after incubation of Western blot membrane with total PKD1-Antibody. It has a pattern opposed to the upper band of 115 kDa where it is higher expressed during HFD and lowers upon ND. However, the physiological meaning of this process requires further investigation.

4.3 Localization of PKD1 in adipocytes

Function and activity status of PKD1 is associated with its localization within the cell [31, 36]. Distribution of PKD1 within the cell in context of function has been investigated in human epithelial cells derived from cervix carcinoma (HeLa cells), rat mammary adenocarcinoma cells (MTLn3 cells, [47]), pancreatic ductal adenocarcinoma cells (Panc89 cells, [49]), colorectal cancer cells (HCT116 and SW480, [81]), dopaminergic neuronal cells (N27, [52]), mouse B-cell and T-cell lymphoma cells (A20 and EL4)[57], amongst others. Overexpressed GFP-tagged PKD1 was found to be localized at TGN and perinuclear in 3T3-L1 adipocytes before [82].

Here, an approach was used to analyze distribution of PKD1 within adipocytes in different activation modes of the kinase. Therefore, 3T3-L1 adipocytes were transfected with plasmids overexpressing PKD1 as wild type, constitutively active, and as kinase that cannot be phosphorylated and therefore not activated (kinase dead) next to regular PKD1 expression. Nucleus of cells was visualized in blue, protein of expressed plasmids in green.

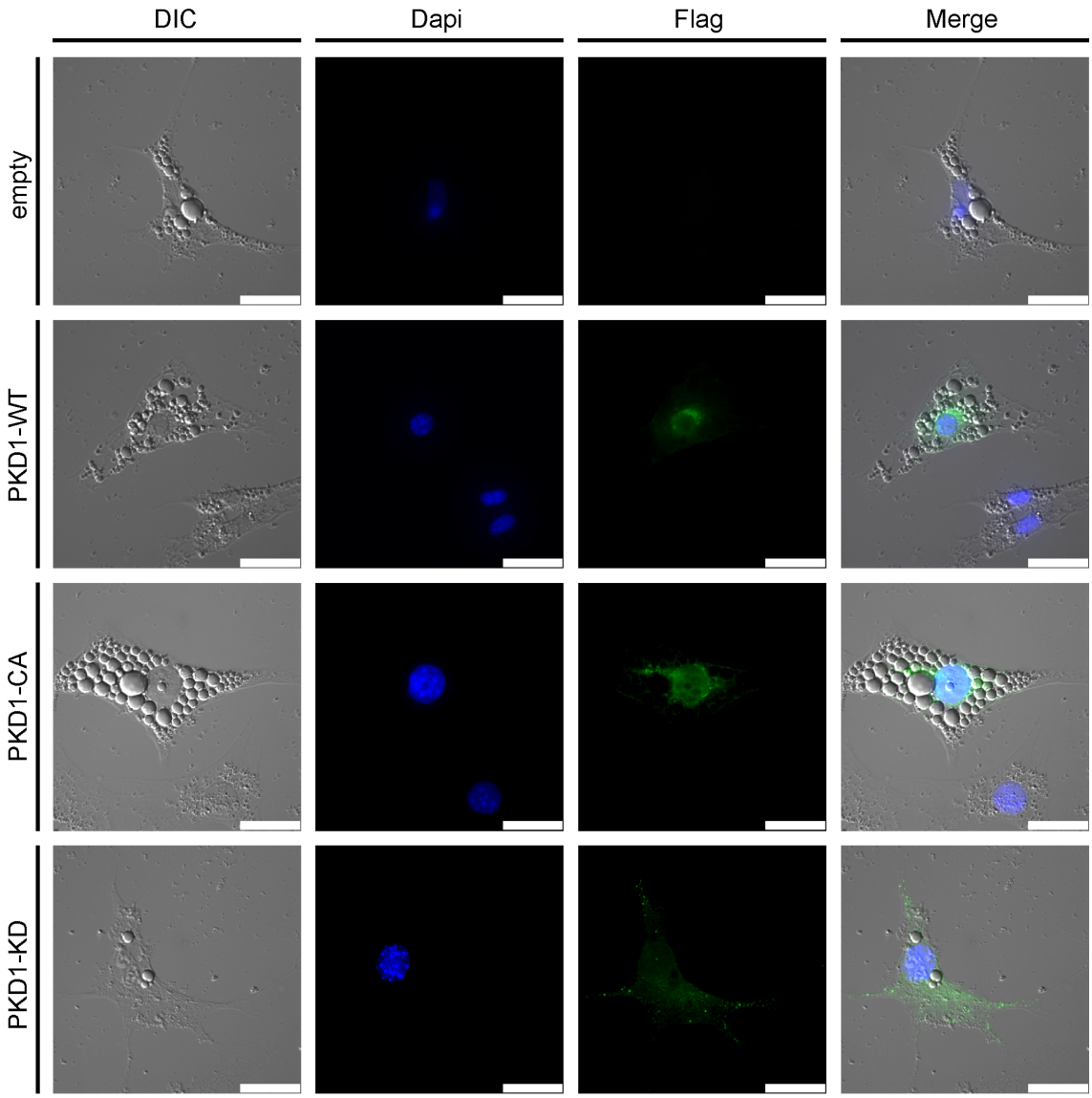

Figure 10: PKD1 localization changes in 3T3-L1 adipocytes depending on PKD1 activity status. In this immunofluorescence analysis, cells were transfected with plasmids containing flag-tagged control (empty), wildtype PKD1 (PKD1-WT), constitutively active PKD1 (PKD1-CA), or kinase-dead PKD1 (PKD1-KD). After 24 hours, proteins were detected with anti-flag primary antibody and alexa fluor® 568 conjugate secondary antibody (green). Nuclei were stained with dapi mounting medium (blue). Differential interference contrast (DIC) visualizes cell shape. All three channels are presented separately and as overlay image (merge). Scale bars represent 25 µm.

Control adipocytes with plasmids expressing nonfunctional protein depicted no flag-tagged protein (Figure 10, empty). Expression of wild type PKD1 led to perinuclear accumulation with emphasis on one side (Figure 10, PKD1-WT). Furthermore, constitutively active form of PKD1 was located peri- as well as intranuclear with little fluorescent signal at the cell periphery (Figure 10, PKD1-CA). PKD1 has been shown to be

involved in vesicle fission at trans-golgi-network (TGN), an organelle associated with perinuclear position, too [42]. Furthermore, this experiment showed that kinase dead PKD1 was scattered mostly in cytoplasm with irregular pattern (Figure 10, PKD1-KD). This is accordant with findings in resting cells, where PKD1 is predominantly found in the cytosol and translocates to organelles when stimulated [30, 31]. Collectively, these results display that association of PKD1 activity with translocation of PKD1 in 3T3-L1 adipocytes can be found.

Interestingly, different patterns of fat vacuole formation within the cell can be observed. Adipocytes transfected with plasmids expressing constitutively active PKD1 depicted many big evenly shaped round fat vacuoles (Figure 10, PKD1-CA), whereas PKD1 wild type and control adipocytes showed fat vacuoles in diverse size and shape (Figure 10, empty and PKD1-WT). In contrast, adipocytes transfected with kinase dead PKD1 contained only few fat droplets (Figure 10, PKD1-KD). Thus, dependency of PKD1 activity status on fat content in adipocytes could be observed. This indicates that either active PKD1 supports lipogenesis and fat accumulation in adipocytes or that PKD1s inactivity leads to an increased rate of lipolysis and/or decreased lipogenesis rate.

4.4 Impact of PKD1 deletion in adipocytes on lipolysis

After visualizing overexpressed PKD1, next the impact of lack of PKD1 in murine adipocytes on lipolytic behavior of these cells was analyzed. PKD1 was transcriptionally down regulated upon the physiological stage of lipolysis during fasting and in contrast it was higher expressed during free food consumption (4.1) as well as during a high fat stage in mice compared to mice on chow diet (4.2). Also, the activated form of PKD1 was mainly localized in and around the nucleus of murine 3T3-L1 adipocytes that also contain filled fat vacuoles (4.3). To determine whether the absence of PKD1 results in altered rate of lipolysis in mouse adipose tissue G. Sumara research group generated $PKD1_{adipo.\Delta/\Delta}$ mice with PKD1 knockout specifically in white adipose tissue.

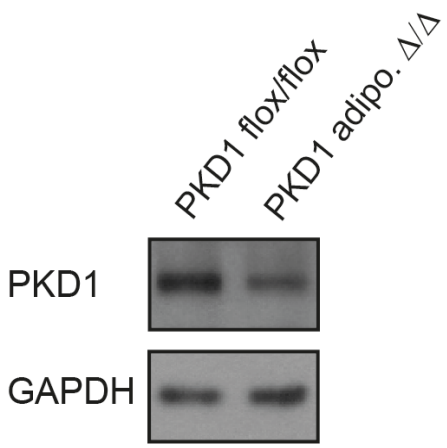

Figure 11: Deletion of PKD1 in mouse epiWAT was efficient. PKD1 floxed mice were cross-bred with mice expressing adiponectin promotor-driven Cre recombinase to generate mice deficient of PKD1 in adipose tissue. EpiWAT was taken from mice expressing PKD1 (PKD1flox/flox, n=4) and lacking PKD1 expression (PKD1adipo. Δ/Δ, n=4) and deletion efficiency was analyzed by Western blot.

Western blot shows that deletion of PKD1 in epiWAT of mice was efficient (Figure 11). Furthermore, lipolysis assay was conducted with epiWAT of PKD1flox/flox and PKD1adipo.Δ/Δ mice fed ND (Figure 12).

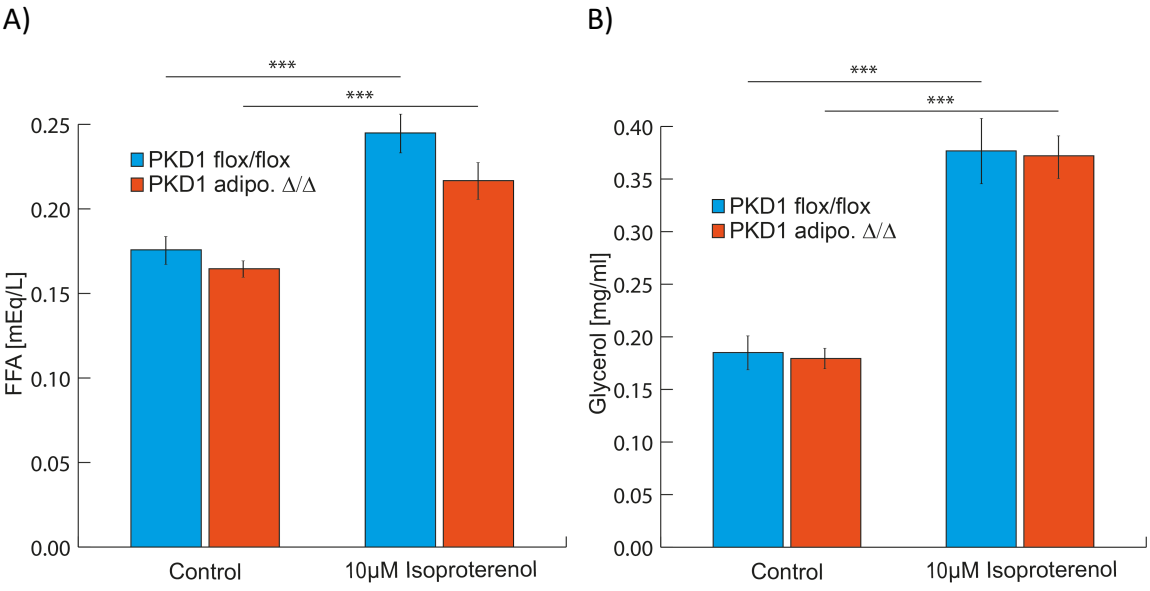

Figure 12: PKD1 deficiency did not affect induced lipolysis in epiWAT from mice. PKD1flox/flox and PKD1adipo.Δ/Δ epiWAT explants were starved in medium for 2 hours. Explants were either further incubated in starvation medium (control) or stimulated with medium containing 10 µM isoproterenol for 2 hours. Lipolysis rate was estimated by measuring FFA (A) and glycerol (B) levels in the medium. For FFA measurements, PKD1 flox/flox control n=10 and stimulated n=11. For glycerol measurements, PKD1 flox/flox control n=10 and stimulated n=12. For FFA and glycerol measurement, PKD1adipo.Δ/Δ control and stimulated n= 13.

Basal FFA and glycerol levels did not reveal differences between PKD1$^{flox/flox}$ and PKD1$^{adipo.\Delta/\Delta}$ (Figure 12, control). Upon isoproterenol stimulation lipolytic products increased in medium of both, PKD1 expressing and PKD1 deficient epiWAT (Figure 12, 10 µM Isoproterenol). Hence, lipolysis in PKD1$^{adipo.\Delta/\Delta}$ epiWAT was not enhanced at basal rate nor when stimulated with isoproterenol compared to wild type epiWAT. Therefore, PKD1 did not affect lipolysis or generation of its products in epigonadal adipose tissue of mice.

4.5 Browning of white adipocytes in PKD1 deficient adipose tissue

Absence of PKD1 in adipose tissue of PKD1$^{adipo.\Delta/\Delta}$ mice fed ND did not affect lipolysis rate (4.4). However, former experiments performed by G. Sumara research group suggest that PKD1$^{adipo.\Delta/\Delta}$ mice fed HFD not only gained less weight in comparison to wild type mice on HFD (Figure 3, A) but also present higher energy expenditure (Figure 3, D and E). Moreover, these mice have significantly lower FFA-levels in peripheral blood than wild type mice (Figure 3, F). FFA are source of energy from lipolysis during times of low calorie intake [14]. It is arguable whether these findings result from higher FFA consumption in cells of mice lacking PKD1 in white adipocytes or from increased FFA consumption in other organs. It was shown before that increase of oxygen consumption and loss of bodyweight due to stimulation of A_{2A} receptors in murine white adipose tissue can be attributed to elevation of browning markers in these cells [83]. Therefore, another possible explanation for low peripheral FFA levels in association with diminished PKD1 expression was addressed. In the next experiment, thermogenic markers that can be found in brown adipose tissue were determined. Expression levels in murine white adipose tissue of PKD1$^{flox/flox}$ and PKD1$^{adipo.\Delta/\Delta}$ mice fed with HFD were compared using RT-qPCR (Figure 13).

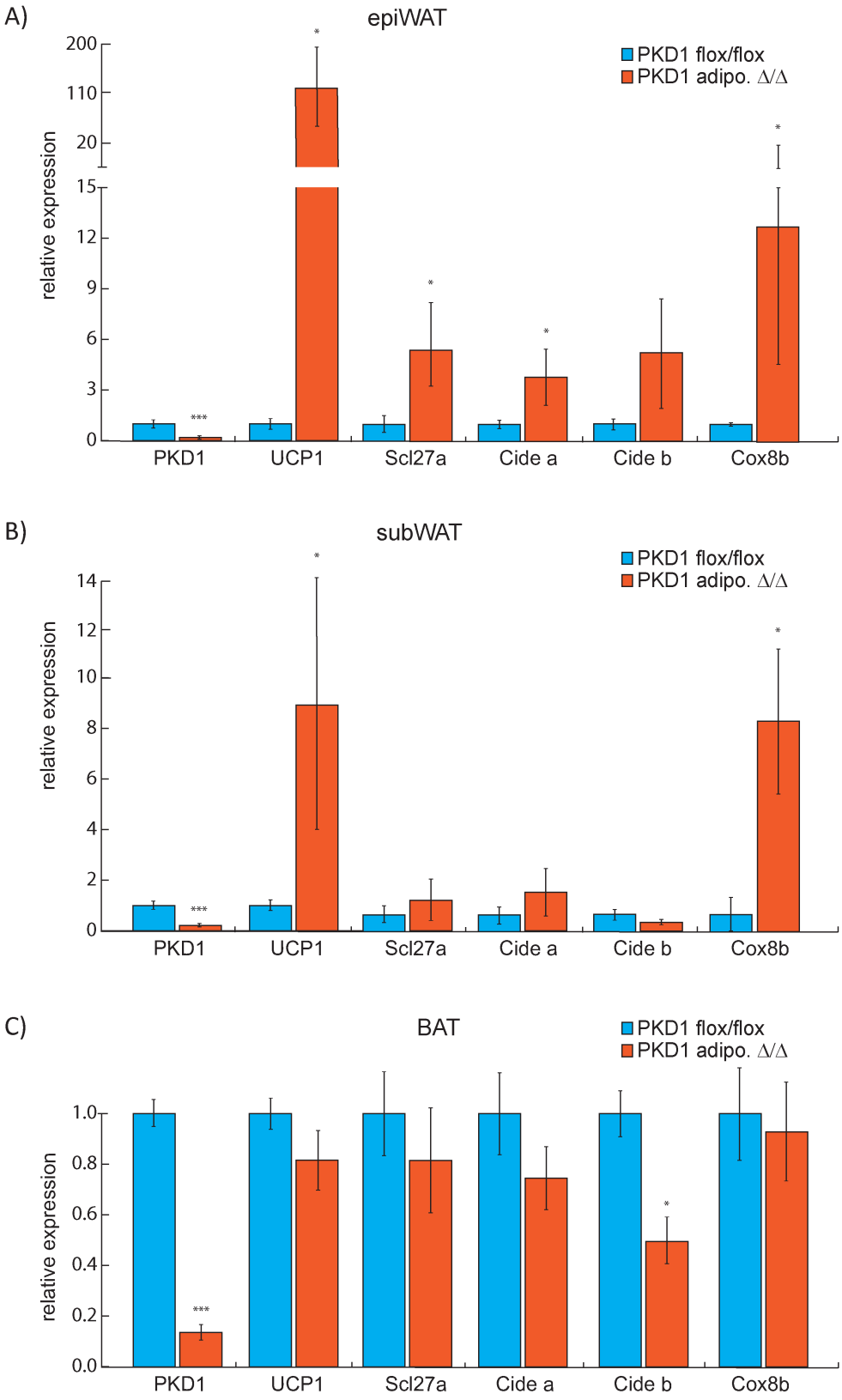

Figure 13: PKD1 deficiency in adipose tissue resulted in elevated expression of marker for browning. RT-qPCR analysis of genes in epigonadal (epiWAT, A) and subcutaneous white adipose tissue (subWAT, B in comparison to brown adipose tissue (BAT, C) from PKD1 flox/flox (n=6) and PKD1 adipo. Δ/Δ (n=5) mice fed with HFD for 24 weeks.

Next to UCP-1, which is the determining protein of brown and beige adipocytes, Cidea and Slc27a, too, represent marker for browning or beiging of white adipose tissue [84, 85]. Cideb is a protein also expressed in BAT and associated with diet-induced obesity [86]. Cox8b is a mitochondrial structural gene and also linked to browning effect [87, 88].

Measurements of PKD1 RNA levels confirmed efficiency of PKD1 knockout in adipose tissue. Results were statistically significant for epiWAT, subWAT and BAT. Strikingly, PKD1$_{adipo.\Delta/\Delta}$ epiWAT depicted over 110-fold higher expression of UCP1, indicating that browning or beiging of white adipocytes and higher energy dissipation took place (Figure 13, A). Also browning marker genes Scl27a (approx. 5.4-fold), Cidea (approx. 3.8-fold), Cideb (approx. 5.2-fold), and Cox8b (approx. 12.7-fold) were elevated in epiWAT. Except for Cideb all values are statistically significant. In subWAT of PKD1$_{adipo.\Delta/\Delta}$ mice, UCP-1 (approx. 8.9-fold) and Cox8b (approx. 8.3-fold) were significantly increased compared to subWAT of wild type mice (Figure 13, B). Other browning marker remained almost unchanged in subWAT. However, this data suggests that browning was not only induced in epiWAT but also in subWAT. Of note, that subcutaneous fats' predominant function is to isolate body from loss of temperature to environment and beige adipocytes are found mainly in subcutaneous WAT [2, 5]. In comparison, UCP1 and other BAT-specific genes remain almost unchanged in of PKD1$_{flox/flox}$ and PKD1$_{adipo.\Delta/\Delta}$ brown adipose tissue of mice fed with HFD (Figure 13, C). Only Cideb is significantly reduced in BAT lacking PKD1.

Thus, selective deletion of PKD1 in mouse adipose tissue induced browning or beiging of white adipocytes in epigonadal and subcutaneous adipose tissue.

5 Discussion

The key functions of PKD1 in many diverse physiological and pathophysiological processes in vertebrates have been described and discussed before [30, 36-38, 62], (1.2.1). Studies focusing on metabolism discovered the importance of PKD1 in metabolic processes: Sumara et al. revealed that active PKD1 enhances insulin secretion from pancreatic β-cells and thus protects from glucose intolerance [42]. A genome-wide association study using significance SNPs, found association of PKD1 gene-locus with BMI [68]. Results of M. Löffler in G. Sumara research group indicated that PKD1-deficiency specifically in adipose tissue protects against HFD-induced obesity (Figure 3, A) and leads to elevated energy expenditure in mice (Figure 3, D and E). However, the specific metabolic function of PKD1 in adipocytes has not been fully understood. Also, physiological mechanisms regulating PKD1 activity in adipocytes are still not known. Elucidating these was the aim of this study.

This study showed that PKD1 activity and expression in white adipose tissue is dependent on the nutritional status of mice. Specifically, expression, protein abundance and activity of PKD1 is down regulated during fasting (4.1.1). Of note, results of this study indicate that expression of PKD1 is not depending on the induction of lipolysis and its products but only on β-adrenergic stimulation of adipocytes (4.1.2), which is a primary signal inducing fasting program in adipocytes [15, 20]. However, reduction of β-adrenergic stimulated lipolysis did not affect the expression of PKD1 (4.1.3). Subsequently, this study showed that consumption of high caloric nutrients induced expression of PKD1 RNA but paradoxically did not induce higher levels of PKD1 protein in epiWAT of mice (4.2). Furthermore, the results presented here indicate that action of PKD1 in adipocytes is regulated not only on the transcriptional level but is also affected by its intracellular distribution. This study showed that activated PKD1 was distributed primarily around the nucleus, while inactive PKD1 presented perinuclear and nuclear localization in murine adipocytes (4.3). In addition to unraveling how activity of PKD1 is regulated, the study investigated its impact on aspects of adipocyte physiology. Specifically, the obtained results indicate that PKD1 did not regulate β-adrenergic stimulated lipolysis (4.4). However, this study showed

that deletion of PKD1 in white adipocytes induced expression of genes implicated in regulation of adaptive thermogenesis in these cells (4.5).

PKD1 expression and activation is suppressed under fasting conditions

One goal of this study was to identify the physiological mechanisms regulating PKD1 expression and activity in white adipocytes. This study demonstrated that fasting of mice significantly reduced expression of PKD1 as well as phosphorylation and therefore activation of PKD1 in white adipocytes (Figure 4).

Fasting is a physiological condition under which stimulation of the sympathetic nervous system is necessary for survival of living organisms to increase lipolysis. Catecholamines trigger signaling cascades at β-adrenergic receptors in adipose tissue in response to food deprivation or fasting finally leading to lipolysis in these cells [20, 89]. This process can be imitated by isoproterenol [90]. The present study displayed that 12 h of fasting of mice, as shown in 24 h, led to reduction of PKD1 RNA and protein levels in white adipose tissue (Figure 4). Moreover, the results demonstrated that isoproterenol stimulation induced generation of lipolytic products in murine white adipose tissue as well as in 3T3-L1 adipocytes and the same stimulation lowered expression of PKD1 in these cells (Figure 5, Figure 6). This indicates involvement of PKD1 in the process of lipolysis.

Wang et al. showed that the transcription factor peroxisome proliferator-acitvated receptor δ (PPARδ) plays a pivotal role in release of TGs and β-oxidation in adipose tissue [91]. Furthermore, Iglesias et al. identified that deletion of PPARβ/δ in pancreatic β-cells leads to an enhanced PKD1 expression and protein activation, indicating regulatory effect of PPAR on PKD1 [92]. Several FFA derivatives act as endogenous agonists for PPARδ transcription and activity [93]. Takahashi et al. suggested that fasting could generate FFA acting as ligands for PPARδ in muscle cells and inducing expression of genes implicated in β-oxidation [94]. Therefore, assumably PKD1 RNA levels could be decreased in fasted adipocytes because of increased abundance of FFAs, which activate PPARδ to suppress PKD1 transcription. However, results of the study presented here showed that inhibition of lipolysis and generation

of its products by knocking down ATGL lipase did not normalize PKD1 expression levels under basal nor under isoproterenol-stimulated condition (Figure 8). This indicates that isoproterenol lowered PKD1 expression in adipocytes independently from TG lipolysis.

Interestingly, transcriptional PPARγ coactivator 1α (PGC-1α) found mainly in brown but also in white adipose tissue to support metabolic gene expression such as UCP-1, can also be activated by β-adrenergic stimulation [20, 95]. In this mechanism, catecholamines bind β-adrenergic receptors enhancing cAMP levels and activity of protein kinase A (PKA). On one the hand, PKA phosphorylates cAMP element binding protein (CREB) transcription factor to induce PGC-1 gene expression. On the other hand, cAMP activates MAP kinase p38α to phosphorylate and excite PGC-1α activity which finally coactivates PPARγ in metabolic gene expression [20]. Transcription factor PPARγ plays a pivotal role in lipid and glucose metabolism and adipocyte differentiation and is found especially in adipocytes [96]. Thus, β-adrenergic activation of PGC-1α and PPARγ could be possible mechanisms explaining reduced PKD1 expression under isoproterenol stimulation of white adipocytes in the experiments conducted in this study. However, Motillio et al. showed that accumulation of lipolytic products in white adipocytes upon β-adrenergic stimulation lead to lower PKA-mediated expression of PGC-1α and UCP-1 mRNA level [97]. This stands in contrast to findings presented in this study, that ATGL silencing and suppression of lipolysis had no impact on PKD1 expression. Therefore, further analysis on FFA-dependent and –independent regulation of PKD1 expression is necessary to understand upstream mechanisms in this process. Also, dependency of PKD1 gene expression on PGC-1α and PPARγ in adipocytes needs to be further investigated.

In the expression of PKD1, PKD1 promoter is crucial and can be epigenetically regulated [98, 99]. Ay et al. revealed that inhibition of histone deacetylase (HDAC) increases PKD1 promoter activity and PKD1 expression [98]. Also, inhibition of methylation of PKD1 promoter at CpG-islands increased PKD1 expression. Furthermore, they identified PKD1 promoter in MN9D dopaminergic neuronal cells as TATA-less and GC-rich and they showed that transcription factors Sp3 and nucelar factor κB (NF-κB) bind and increase the promoters' activity [98]. NF-κB was shown to

be activated upon nutrient excess and promote metabolic diseases [100]. Interestingly, short-term calorie restriction was shown to inhibit NF-κB expression and DNA binding activity in rat kindeys [101]. Thus, fasting of mice in the experiment presented here could hypothetically lower NF-κB levels and therefore attenuate PKD1 promoter activity. Possibly, reduction of PKD1 expression in fasted mice of this study resulted from downregulation of transcription factor NF-κB.

The kinase function of PKD1 is activated when phosphorylated [30]. Apart from PKD1 RNA levels, this study showed that phosphorylation and therefore activity of PKD1 is reduced in WAT upon fasting of mice (Figure 4, A and B, PKD1-Ser916), a process that induces lipolysis and generation of lipolytic products [14]. Furthermore, Western blot showed that not only PKD1-Ser916 but also total PKD1 was downregulated upon fasting. Therefore, it is unclear whether PKD1 was downregulated only as a result of attenuated transcription or if other mechanisms reduced PKD1 activity as well.

DAG acts as secondary messenger of cell surface receptors to bind and activate PKD [30]. Thus, the question arises if DAGs derived from TG lipolysis have potential to activate PKD1, too. However, this study showed that fasting did not stimulate PKD1 activity but induce the opposite (Figure 4, A and B, PKD1-Ser916). It has been discussed before that lipolysis of TGs by ATGL display DAGs with stereoisomeric (1,3-DAG and 2,3-DAG) and locational differences to 1,2-DAG which serves as signaling mediator and activator of PKC [15].

Furthermore, GPCR is activator of the DAG-PKC-PKD-signaling pathway [37]. As mentioned before, WAT is innervated by sympathetic nervous system, which induces lipolysis during fasting through β-adrenergic receptor, a GPCR [20]. Therefore, it seems contrary that fasting induced downregulation of PKD1 activity in adipocytes. However, it was observed in cardiomyocytes that PKD1 is only activated by GPCR agonists when coupling to G_q α-subunit, but not by β-adrenergic receptors, that couple G_s and G_i subunits of GPCR [102].

Therefore, regulation of PKD1 activity during fasting is rather caused by transcriptional downregulation of PKD1 as discussed above.

In summary, these results support the hypothesis that PKD1 expression is dependent on the physiological metabolic process of fasting in white adipocytes. PKD1 RNA and protein levels were downregulation in adipose tissue of fasted mice. PKD1 expression is possibly regulated by transcriptional mechanisms in which transcription factor PPARγ and coactivator PGC-1α in context of β-adrenergic stimulation, or epigenetic mechanisms and NF-κB at PKD1 promotor could play a role. However, the precise mechanism behind the findings and the role of isoproterenol stimulation in context of PKD1 expression need to be further evaluated and invite to future experiments.

Adiposity in mice is linked to high levels of PKD1 in white adipocytes

The second focus to understand physiological mechanisms regulating PKD1 expression and activation in white adipocytes was put on the state of food abundance under which lipogenesis and adipogenesis take place in adipocytes. On the one hand, lipogenesis leads to fat accumulation and subsequently to hypertrophy of adipocytes, on the other hand adipogenesis generates hyperplasia of adipose tissue, subsequently leading to body weight gain [1].

Results of M. Löffler from G. Sumara research group showed that mice deficient for PKD1 in adipose tissue are resistant to HFD-induced obesity and also display lower peripheral FFA levels (Figure 3, A and F). This study showed that epiWAT of HFD-induced obese mice displayed significantly increased PKD1 expression in RT-qPCR (Figure 9, A). Also, re-feeding of fasted mice enhanced PKD1 RNA expression and protein activity in white adipose tissue (Figure 4). Furthermore, in the in vitro model, in which transfection with plasmids led to overexpression of constitutively active PKD1, 3T3-L1 adipocytes displayed a phenotype with many filled fat vacuoles whereas adipocytes expressing non-functional PKD1 (PKD1-KD) showed poorer fat accumulation, indicating that PKD1 supports fat accumulation in 3T3-L1 adipocytes, too (Figure 10). Therefore, it seems likely that PKD1 plays an important role in the process of adaptation to food abundance in adipocytes.

In the process of adipogenesis as well as lipogenesis and TG storage, PPARγ is the pivotal transcription factor that activates gene expression of proteins involved in these processes [96]. PPARγ is mainly found in WAT and activation by PPARγ agonist thiazolidinediones (TZD) was shown to lower TNF-alpha and peripheral FFA levels due to flux into WAT, hence supporting insulin sensitivity, and also increase WAT mass due to adipogenesis [103]. Regular PPARγ activation led to high TG content in WAT, obesity in mice as well as increase of insulin resistance in response to HFD [103]. Furthermore, PPARγ-deficiency protected from HFD-induced obesity due to decrease in lipogenesis so that WAT displayed decreased TG content [103]. Possibly, PKD1 underlies transcriptional regulation of PPARγ in in the process of adipogenesis and lipogenesis in response to HFD.

As mentioned before, study in neuronal cells showed that PKD1 promoter is activated by NF-κB among other transcriptional factors [98]. A recent study revealed that NF-κB, regulated by KRas, binds to PKD1 promoter and enhances PKD1 expression in pancreatic cancer cells [104]. NF-κB is a transcriptional factor involved in the processes of inflammation and development of metabolic diseases [100]. It was shown that HFD induces NF-κB activity in adipose tissue [105]. This suggests that high PKD1 levels in WAT of mice on HFD in this study might be mediated by HFD-induced activity of NF-κB. Interestingly, it was also shown that in response to oxidative stress PKD1 activates NF-κB through IκB-kinase β (IKKβ) of the IKK-complex and thus promotes cell survival [51]. Therefore, PKD1 and NF-κB might function in an amplification signaling loop in HFD-induced WAT expansion, as described before in pancreatic cancer [104]. Hence, high PKD1 RNA levels in HFD-induced obese mice of this study might also underlie regulation of PKD1 promoter through NF-κB activity. Thus, regulatory role of NF-κB on PKD1 and wise versa in obesity display an interesting target for further research in development and treatment of obesity and metabolic diseases.

Taken together, results of this study strongly suggest involvement of PKD1 in regulatory mechanisms directing fat accumulation in WAT, making PKD1 an interesting

target for metabolic disease therapy. Expression of PKD1 in response to food abundance possibly include the transcription factor PPARγ or HFD-induced activation of NF-κB. Their interaction in adipocytes upon HFD could be focus of future experiments. Elucidating mechanisms inhibiting growth and expansion of white adipocyte tissue may offer attractive possibilities for therapeutic prevention of development of obesity and related diseases in the future [1].

Upon HFD, PKD1 protein depicts low molecular weight in Western Blotting

Next to PKD1 RNA levels, this study examined PKD1 protein activity in HFD-exposed mice using Western blot (Figure 9, B). Surprisingly, PKD1 protein levels were upregulated in epiWAT of mice fed ND and downregulated when fed HFD, which is contrary to RT-qPCR results of PKD1 RNA levels (Figure 9, A). However, total PKD1 protein detection also exhibited a band at approximately 90 kDa, which has a pattern opposed to the upper band of 115 kDa. The 90 kDa band is stronger in epiWAT of mice fed HFD and lowers upon ND. This might indicate that in response to HFD PKD1 undergoes posttranslational modification or is alternatively transcribed to produce a lower molecular weight form in WAT.

Increased food intake and obesity are known to induce hypertrophy and hyperplasia of adipocytes, that can cause hypoxia and macrophage invasion [1, 9, 28, 106]. Furthermore, adipocyte hypertrophy due to obesity in mice leads to pro-apoptotic gene expression and eventually to cell apoptosis in white adipose tissue through the actions of caspase 3 amongst others [107, 108]. During induction of apoptosis caspase 3 was found to cleave PKD1 in the C1-PH interdomain generating active PKD1 fragments [109, 110]. This led to consideration whether low molecular weight of PKD1 in hypertrophic adipose tissue of HFD fed mice could be due to cleavage and activation of PKD1 in these cells. In neurons, oxidative stress was shown to activate PKD1 in a PKC-dependent manner and protect neuronal cells from apoptosis [52]. Hence, in neurons PKD1 showed anti-apoptotic function [52], whereas caspase 3, besides activating PKD1 [110], mediates apoptosis in hypertrophic adipocytes of diet-induced obese mice [107]. Thus, hypothetically PKD1 could have regulatory attributes, being

activated by and acting as opponent of caspase 3, and in this study, increase of PKD1 at 90 kDA in Western blot obtained from epiWAT of HDF fed mice could be explained by anti-apoptotic function of PKD1 in hypertrophic white adipose tissue. However, there are certain disagreements to consider. First, Asaithambi et al. detected cleaved product of PKD1 at a size of approximately 60 kDa [52], a smaller protein than the protein detect in this study. Vantus et al. additionally found a PKD1 fragment at 100 kDA after incubation with caspase-3, -6, -8 or -11 showing that other caspases might also process PKD1 [39]. Second, in this study, PKD1-Ser916 presenting the activated form of PKD1, is stronger detected in Western blot of adipose tissue from mice fed with ND and not HFD (Figure 9, B). And third, besides posttranslational protein modification, in the process of gene transcription alternative splicing might also produce a protein of other molecular weight and function [111, 112].

Therefore, the exact mechanism leading to the behind low molecular weight of PKD1 adipocytes upon HFD could not sufficiently be explained. However, this result gives an impulse for research on alternative ways to activate PKD1. Especially, because inflammation and apoptosis in adipose tissue is associated with metabolic dysfunction [1].

PKD1 activity status, location, and adipocyte phenotype

In the experimental approach of adipocyte transfection and staining, correlation between activity status of PKD1, its localization within 3T3-L1 adipocytes and the phenotype these cells exhibit was analyzed (Figure 10). It is known that biological effect of PKD1 is linked to its intracellular localization [36-38]. Here, we show that non-functional PKD1 (PKD1-KD) is predominantly found in the cytoplasm of 3T3-L1 adipocytes (Figure 10), as it is known of inactive PKD1 in resting cells [30, 31]. Interestingly, PKD-KD transfected cells contain only few fat vacuoles compared to the control adipocytes indicating that an enhanced TG lipolysis took place or lipogenesis was suppressed. Moreover, PKD1-WT and PKD1-CA accumulate perinuclear and intranuclear in adipocytes where the latter display many round fat vacuoles, suggesting that enhanced fat accumulation occurred (Figure 10, PKD1-WT and -CA). This

is concordant with RT-qPCR results of HDF-induced obese mice, where PKD1 was highly expressed (Figure 9). Recent study in muscle cells identified a novel upstream target of PKD1: It phosphorylates and therefore inactivates AMP-activated protein kinase (AMPK) at its α2 subunit [113]. AMPK is involved in regulation of energy homeostasis in adipocytes and inhibits anabolic processes such as TG synthesis. When Acetyl-CoA carboxylase, a target of AMPK, is phosphorylated by the kinase, lipogenesis is inhibited in adipocytes [114]. Hence, PKD1 activity possibly supports lipogenesis and therefore fat accumulation in adipocytes through suppression of AMPK as seen in the presented results. This signaling cascade is an interesting subject for further research in future experiments.

Furthermore, activated PKD1 is known to translocate to nucleus and also presents perinuclear localization [30]. PKD1 regulates vesicle fission from TGN, which is located perinuclear [59]. Study in pancreatic β-cells showed that PKD1 activity at TGN led to insulin vesicle fission and insulin secretion [42]. Other study in 3T3-L1 adipocytes suggested that PKD1 activity could partially regulate leptin vesicle trafficking at TGN, as a kinase dead mutant resulted in significant decrease of leptin secretion [82]. Therefore, PKD1 assumably supports TGN trafficking to plasma membrane in adipocytes and possibly contributes to adipocyte endocrine function, too.

In nucleus, PKD1 is known to regulate transcription through the actions of class-IIa HDAC [37]. In epithelial cells, active PKD1 was shown to translocate of PKD1 into the nucleus where it regulates HDAC5 localization and phosphorylation [41]. Thus, nuclear accumulation of PKD-WT and PKD-CA indicate that activated PKD1 enhances gene transcription in adipocytes.

However, besides nucleus no other cellular organelle was stained in this experiment, so that position of PKD1 in adipocytes cannot directly be related to specific localization. Also, in this experimental approach quantitative measurement of fat content in adipocytes was not performed. Therefore, a precise conclusion about phenotype and fat content in adipocytes is not possible but a tendency can be observed. Hence, this experimental approach supports the assumptions drawn from

other experiment results in this study and gives reason for further investigation on PKD1 in adipocytes. In future experiments, lipid droplets could be stained using using Oil-Red-O to visualize, measure, and quantify intracellular lipid droplets in microscope images.

PKD1 ablation in white adipose tissue does not have an impact on isoproterenol-induced lipolysis but induces browning of these cells

Focus of this study was not only the identification of physiological conditions regulating PKD1 but also testing PKD1-dependency on mechanisms regulating energy expenditure in murine adipocytes. In G. Sumara research group, M. Löffler was able to show that PKD1$^{adipo.\Delta/\Delta}$ mice fed with HFD gained less weight than wild type littermates (Figure 3, A, PKD1$^{adipo.\Delta/\Delta}$ and PKD$^{f/f}$ HFD). In this study, 3T3-L1 adipocytes over-expressing PKD1-KD displayed only little fat accumulation (Figure 10). This indicates involvement of PKD1 in regulation of proteins or enzymes promoting energy expenditure.

In adipocytes, lipolysis of TG is one of the main processes of lipid energy metabolism [14], and therefore was the first mechanism tested in this study. However, deletion of PKD1 in white adipose tissue of mice fed with ND had neither an impact on generation of lipolytic products at basal status nor was the lipolysis rate different to wild type adipose tissue when stimulated with isoproterenol (Figure 12). Hence, isoproterenol, which is known to induce lipolysis in adipocytes [115], acts as a potent stimulator on adipose tissue of mice fed ND independently from PKD1. This finding is consistent with results of M. Löffler which revealed no difference in body weight gain of PKD1$^{adipo.\Delta/\Delta}$ and PKD1$^{flox/flox}$ mice when fed with ND (Figure 3, A, PKD1$^{adipo.\Delta/\Delta}$ and PKD1$^{f/f}$ ND).

Furthermore, in the study of M. Löffler mice fed with ND did not develop obesity in comparison to mice fed with HFD (Figure 3, A). In fact, consumption of energy-dense food high in fat is the main reason for obesity and metabolic disease in high- and middle-income countries, next to physical inactivity [23]. To balance energy equation, excessive calorie-intake needs to be compensated through a higher energy

expenditure. Otherwise the energetic imbalance leads to increased fat accumulation and adipocyte growth [1, 23]. In PKD1$^{adipo.\Delta/\Delta}$ mice fed HFD, M. Löffler measured significantly lower FFA-blood levels as well as increased O_2 consumption and higher CO_2 dissipation than in their wild type littermates (Figure 3, C-E), indicating that PKD1 deletion leads to higher energy expenditure and improved metabolic rate in mice with high caloric food-intake.

Among others, high energy expenditure can be reached by increased exercise where lipolysis of stored TGs takes place, which here was not affected by deletion of PKD1, or through energy dissipation in brown or beige adipocytes through the actions of UCP-1 [1, 5]. In the presented study, deletion of PKD1 specifically in adipocytes led to browning of WAT in mice fed with HFD (4.5). UCP-1, most important marker for brown and beige adipocytes [5], was increased in epiWAT PKD1$^{adipo.\Delta/\Delta}$ over 110-fold compared to PKD1$^{flox/flox}$ epiWAT, and in subWAT UCP-1 expression was 8.9-fold higher in PKD1$^{adipo.\Delta/\Delta}$ than in PKD1$^{flox/flox}$ subWAT (Figure 13, A and B). Both results were statistically significant. Additionally, other browning markers such as Slc27a, Cidea, and Cox8b [84-87] were significantly elevated in PKD1$^{adipo.\Delta/\Delta}$-epiWAT and Cox8b in PKD1$^{adipo.\Delta/\Delta}$-subWAT (Figure 13, A and B). Expression of those genes was not affected in PKD1$^{flox/flox}$ and PKD1$^{adipo.\Delta/\Delta}$ BAT of mice fed with HFD (Figure 13, C). Together, these findings demonstrate that deletion of PKD1 in adipocytes led to browning in epigonadal and subcutaneous WAT without affecting BAT. Browning or beiging is a process which is sufficient to increase energy expenditure and suppress diet-induced body weight gain [1, 5]: Seale et al. showed that transgenic expression of brown adipose tissue determination factor Prdm16 in WAT not only induced browning in subWAT by expression of UCP-1 and Cidea among others, but also led to improved energy expenditure in terms of oxygen consumption and inhibited weight gain in mice fed HFD [116]. Furthermore, Gnad et al. discussed that increase of oxygen consumption and loss of body weight due to stimulation of A_{2A}-receptors in murine white adipose tissue can be attributed to elevation of browning markers in these cells, too [83]. Concordant with that, expression of UCP-1 in this study could explain higher

energy dissipation and suppression of HFD-induced weight gain in PKD1adipo.Δ/Δ-mice in the study of M. Löffler (Figure 3, A, D and E).

In this study, browning marker were determined in WAT of mice fed HFD, but not when fed ND, because inhibitory effect of PKD1 deletion in adipocytes on body weight gain in M. Löfflers results was observed under HFD feeding of (Figure 3, A). Therefore, a separate conclusion to WAT in mice fed with ND cannot be drawn and could be subject of future experiments. Also, browning-marker and energy expenditure could be analyzed in PKD1-deficient adipocytes in an in vitro experiment, for example as used before in the case of Prdm16 using stroma vascular cells from subWAT of mice transduced with adenovirus expressing shRNA targeted to PKD1 [116]. Not to forget, increased oxygen consumption can be attributed to increased mitochondrial activity and to higher amount of mitochondrial content in adipose tissue of mice, as has been shown by Wilson-Fritch et al. [117]. It would be interesting to investigate differences in respiration rate and mitochondrial content in adipose tissue of PKD1-deficient mice and their wildtype littermates in future experiments.

Another consideration is possible in the context that ablation of PKD1 induced browning in white adipose tissue (4.5) and findings of PKD1 protein detection in epiWAT of mice on HFD (4.2). Possibly, PKD1 is cleaved not with gaining an active status but with loss-of-function in adipose tissue of mice on HDF (Figure 9, B) so that excessive calories can be dissipated through induction of browning at a certain point in time rather than stored. Western blot revealed loss in activity of PKD1 upon HFD, too (Figure 9, B, PKD1-Ser916) and hence, this finding supports the assumption that PKD1 deletion in epiWAT induces browning in this tissue when mice are fed with HFD.

It is known that browning of white adipose tissue can be induced by exposure to cold, β-adrenergic stimulation, and PPARγ-agonist thiazolidinediones (TZD) or mimicked by chemical uncoupler 2,4-dinitrophenol (DNP) [85]. However, these methods are yet unlikely to be used as therapeutic method to reduce body weight in humans, as they entail unpleasant or even life-incompatible side-effects [85]. In fact, TZDs were already

used as pharmaceutical in treatment of T2DM but are associated with body weight gain rather than loss, cardiovascular dysfunction, and others, so that application in humans was strictly limited [118, 119]. Thus, targeting PKD1 function in white adipose tissue in obese could offer a new therapeutic approach to prevent obesity, metabolic syndrome and in consequence prevent diseases in which they serve as major risk factor: Cardiovascular disease, with heart attack and stroke as the worldwide leading causes for death, as well as T2DM [24, 25].

6 Summary

Adipocytes are specialized cells found in vertebrates to ensure survival in terms of adaption to food deficit and abundance. However, their dysfunction accounts for the pathophysiology of metabolic diseases such as T2DM. Preliminary data generated by Mona Löffler suggested that PKD1 is involved in adipocyte function. Here, I show that PKD1 expression and activity is linked to lipid metabolism of murine adipocytes. PKD1 gene expression and activity was reduced in murine white adipose tissue upon fasting, a physiological condition which induces lipolysis. Isoproterenol-stimulated lipolysis in adipose tissue and 3T3-L1 adipocytes reduced PKD1 gene expression. Silencing ATGL in adipocytes inhibited isoproterenol-stimulated lipolysis, however, the β-adrenergic stimulation of ATGL-silenced adipocytes lowered PKD1 expression levels as well.

Adipose tissue of obese mice exhibited high PKD1 RNA levels but paradoxically lower protein levels of phosphorylated PKD1-Ser916. However, HFD generated a second PKD1 protein product of low molecular weight in mouse adipose tissue.

Furthermore, constitutively active PKD1 predominantly displayed nuclear localization in 3T3-L1 adipocytes containing many fat vacuoles. However, adipocytes overexpressing non-functional PKD1 contained fewer lipid droplets and PKD1-KD was distributed in cytoplasm.

Most importantly, deficiency of PKD1 in mouse adipose tissue caused expression of genes involved in adaptive thermogenesis such as UCP-1 and thus generated brown-like phenotype adipocytes.

Thus, PKD1 is implicated in adipose tissue function and presents an interesting target for therapeutic approaches in the prevention of obesity and associated diseases.

7 Zusammenfassung

Adipozyten sind spezialisierte Zellen der Wirbeltiere, die das Überleben durch Anpassung an Nahrungsmangel und Nahrungsüberfluss gewährleisten. Eine Dysfunktion von Adipozyten bedingt jedoch die Pathophysiologie von Stoffwechselerkrankungen wie dem T2DM. Vorläufige Ergebnisse von Mona Löfflers Versuchen zeigten, dass PKD1 in der Funktion von Adipozyten involviert ist.

Innerhalb dieser Arbeit konnte dargestellt werden, dass die Expression und Aktivität von PKD1 in murinen Adipozyten an den Lipidmetabolismus gekoppelt ist. Beim Hungern von murinem weißen Fettgewebe, einem physiologischen Zustand, der Lipolyse induziert, war die Genexpression von PKD1 reduziert. Isoproterenol-stimulierte Lipolyse führte ebenfalls zu verminderter Expression von PKD1 in murinen weißen Fettgewebe und 3T3-L1 Adipozyten. In ATGL-silenced Adipozyten war die Isoproterenol-stimulierte Lipolyse zwar inhibiert, allerdings wurde die Genexpression von PKD1 durch die β-adrenerge Stimulation ebenfalls vermindert.

Fettgewebe von adipösen Mäusen hingegen wiesen hohe PKD1 RNA Level sowie einen niedrigen Proteingehalt der phosphorylierten Form PKD1-Ser916 auf. Fettreiche Ernährung von Mäusen generierte in Fettgewebe jedoch ein weiteres Produkt von PKD1 mit niedrigem Molekulargewicht im Western Blot.

Des Weiteren wurde dargestellt, dass konstitutiv aktives PKD1 in 3T3-L1 Adipozyten vorwiegend nuklear lokalisiert war und diese Adipozyten einen hohen Gehalt von Fettvakuolen aufwiesen. Adipozyten, die funktionsloses PKD1 exprimierten, enthielten wenige Lipidtropfen und PKD1-KD war im Cytoplasma verteilt

Vor allem zeigte diese Arbeit, dass die Deletion von PKD1 spezifisch in murinem Fettgewebe die Expression von Genen wie UCP-1 verursachte, die eine Rolle in adaptiver Thermogenese spielen, und dadurch einen brown-like Phänotypen generierte.

Zusammenfassend ist PKD1 in die Funktionen von Adipozyten verwickelt und stellt ein attraktives Ziel für therapeutische Ansätze in der Prävention von Übergewicht und damit assoziierten Erkankungen dar.

8 References

1. Rosen, E.D. and B.M. Spiegelman, *What we talk about when we talk about fat.* Cell, 2014. **156**(1-2): p. 20-44.
2. Lüllmann-Rauch, R., *Taschenbuch: Histologie*. 5 ed. 2015, Stuttgart: Thieme. p. 146 - 149.
3. Friedl, K.E., et al., *Lower limit of body fat in healthy active men.* J Appl Physiol (1985), 1994. **77**(2): p. 933-40.
4. Tran, T.T., and Kahn, C.R., *Transplantation of adipose tissue and stem cells: role in metabolism and disease.* Nat. Rev. Endocinol., 2010. **6**: p. 195 - 213.
5. Sidossis, L. and S. Kajimura, *Brown and beige fat in humans: thermogenic adipocytes that control energy and glucose homeostasis.* J Clin Invest, 2015. **125**(2): p. 478-86.
6. Cypess, A.M., et al., *Identification and importance of brown adipose tissue in adult humans.* N Engl J Med, 2009. **360**(15): p. 1509-17.
7. Saito, M., et al., *High incidence of metabolically active brown adipose tissue in healthy adult humans: effects of cold exposure and adiposity.* Diabetes, 2009. **58**(7): p. 1526-31.
8. van Marken Lichtenbelt, W.D., et al., *Cold-activated brown adipose tissue in healthy men.* N Engl J Med, 2009. **360**(15): p. 1500-8.
9. Rosen, E.D. and B.M. Spiegelman, *Adipocytes as regulators of energy balance and glucose homeostasis.* Nature, 2006. **444**(7121): p. 847-53.
10. Loeffler/Petrides, *Loeffler/Petrides Biochemie und Pathobiochemie*. 9 ed. 2014, Springer-Lehrbuch: Heinrich, Mueller, Graeve. p. 235-251 (1073).
11. Lowell, B.B., et al., *Development of obesity in transgenic mice after genetic ablation of brown adipose tissue.* Nature, 1993. **366**(6457): p. 740-2.
12. Giralt, M. and F. Villarroya, *White, brown, beige/brite: different adipose cells for different functions?* Endocrinology, 2013. **154**(9): p. 2992-3000.
13. Kazak, L., et al., *A creatine-driven substrate cycle enhances energy expenditure and thermogenesis in beige fat.* Cell, 2015. **163**(3): p. 643-55.
14. Wang, S., et al., *Lipolysis and the integrated physiology of lipid energy metabolism.* Mol Genet Metab, 2008. **95**(3): p. 117-26.
15. Zechner, R., et al., *FAT SIGNALS--lipases and lipolysis in lipid metabolism and signaling.* Cell Metab, 2012. **15**(3): p. 279-91.
16. Schweiger, M., et al., *Adipose triglyceride lipase and hormone-sensitive lipase are the major enzymes in adipose tissue triacylglycerol catabolism.* J Biol Chem, 2006. **281**(52): p. 40236-41.
17. Friedman, J.M., *The function of leptin in nutrition, weight, and physiology.* Nutr Rev, 2002. **60**(10 Pt 2): p. S1-14; discussion S68-84, 85-7.
18. Turer, A.T. and P.E. Scherer, *Adiponectin: mechanistic insights and clinical implications.* Diabetologia, 2012. **55**(9): p. 2319-26.
19. Steppan, C.M. and M.A. Lazar, *The current biology of resistin.* J Intern Med, 2004. **255**(4): p. 439-47.
20. Robidoux, J., T.L. Martin, and S. Collins, *Beta-adrenergic receptors and regulation of energy expenditure: a family affair.* Annu Rev Pharmacol Toxicol, 2004. **44**: p. 297-323.

21. Kreier, F., et al., *Selective parasympathetic innervation of subcutaneous and intra-abdominal fat--functional implications.* J Clin Invest, 2002. **110**(9): p. 1243-50.
22. Spiegelman, B.M. and J.S. Flier, *Obesity and the regulation of energy balance.* Cell, 2001. **104**(4): p. 531-43.
23. Organization, W.H. *Obesity and overweigh*. October 2017; Fact sheet N°311:[Available from: http://www.who.int/mediacentre/factsheets/fs311/en/.
24. Federation, I.D. *The IDF consensus worldwide definition of the metabolic syndrome*. 2006; Available from: https://www.idf.org/our-activities/advocacy-awareness/resources-and-tools/60:idfconsensus-worldwide-definitionof-the-metabolic-syndrome.html.
25. Organization, W.H. *The top 10 causes of death*. January 2017; Fact sheet N°310:[Available from: http://www.who.int/mediacentre/factsheets/fs310/en/.
26. Herold, G.e.a., *Innere Medizin*. Vol. 2018. October 2017. p. 722 - 735 (1000).
27. Organization, W.H. *Diabetes*. November 2017; Fact sheet N°312:[Available from: http://www.who.int/mediacentre/factsheets/fs312/en/.
28. Muir, L.A., et al., *Adipose tissue fibrosis, hypertrophy, and hyperplasia: Correlations with diabetes in human obesity.* Obesity (Silver Spring), 2016. **24**(3): p. 597-605.
29. Wellen, K.E. and G.S. Hotamisligil, *Inflammation, stress, and diabetes.* J Clin Invest, 2005. **115**(5): p. 1111-9.
30. Rykx, A., et al., *Protein kinase D: a family affair.* FEBS Lett, 2003. **546**(1): p. 81-6.
31. Rozengurt, E., O. Rey, and R.T. Waldron, *Protein kinase D signaling.* J Biol Chem, 2005. **280**(14): p. 13205-8.
32. Iglesias, T., R.T. Waldron, and E. Rozengurt, *Identification of in vivo phosphorylation sites required for protein kinase D activation.* J Biol Chem, 1998. **273**(42): p. 27662-7.
33. Steinberg, S.F., *Regulation of protein kinase D1 activity.* Mol Pharmacol, 2012. **81**(3): p. 284-91.
34. Boni, L.T. and R.R. Rando, *The nature of protein kinase C activation by physically defined phospholipid vesicles and diacylglycerols.* J Biol Chem, 1985. **260**(19): p. 10819-25.
35. Baron, C.L. and V. Malhotra, *Role of diacylglycerol in PKD recruitment to the TGN and protein transport to the plasma membrane.* Science, 2002. **295**(5553): p. 325-8.
36. Fu, Y. and C.S. Rubin, *Protein kinase D: coupling extracellular stimuli to the regulation of cell physiology.* EMBO Rep, 2011. **12**(8): p. 785-96.
37. Wang, Q.J., *PKD at the crossroads of DAG and PKC signaling.* Trends Pharmacol Sci, 2006. **27**(6): p. 317-23.
38. Rozengurt, E., *Protein kinase D signaling: multiple biological functions in health and disease.* Physiology (Bethesda), 2011. **26**(1): p. 23-33.

39. Vantus, T., et al., *Doxorubicin-induced activation of protein kinase D1 through caspase-mediated proteolytic cleavage: identification of two cleavage sites by microsequencing.* Cell Signal, 2004. **16**(6): p. 703-9.
40. Kong, K.C., et al., *M3-muscarinic receptor promotes insulin release via receptor phosphorylation/arrestin-dependent activation of protein kinase D1.* Proc Natl Acad Sci U S A, 2010. **107**(49): p. 21181-6.
41. Chang, J.K., et al., *Protein kinase D1 (PKD1) phosphorylation on Ser(203) by type I p21-activated kinase (PAK) regulates PKD1 localization.* J Biol Chem, 2017. **292**(23): p. 9523-9539.
42. Sumara, G., et al., *Regulation of PKD by the MAPK p38delta in insulin secretion and glucose homeostasis.* Cell, 2009. **136**(2): p. 235-48.
43. Sinnett-Smith, J., et al., *Protein kinase D potentiates DNA synthesis induced by Gq-coupled receptors by increasing the duration of ERK signaling in swiss 3T3 cells.* J Biol Chem, 2004. **279**(16): p. 16883-93.
44. Ernest Dodd, M., et al., *Regulation of protein kinase D during differentiation and proliferation of primary mouse keratinocytes.* J Invest Dermatol, 2005. **125**(2): p. 294-306.
45. Jadali, A. and S. Ghazizadeh, *Protein kinase D is implicated in the reversible commitment to differentiation in primary cultures of mouse keratinocytes.* J Biol Chem, 2010. **285**(30): p. 23387-97.
46. Ren, B., *Protein Kinase D1 Signaling in Angiogenic Gene Expression and VEGF-Mediated Angiogenesis.* Front Cell Dev Biol, 2016. **4**: p. 37.
47. Eiseler, T., et al., *Protein kinase D1 regulates cofilin-mediated F-actin reorganization and cell motility through slingshot.* Nat Cell Biol, 2009. **11**(5): p. 545-56.
48. Ziegler, S., et al., *A novel protein kinase D phosphorylation site in the tumor suppressor Rab interactor 1 is critical for coordination of cell migration.* Mol Biol Cell, 2011. **22**(5): p. 570-80.
49. Eiseler, T., et al., *Protein kinase D controls actin polymerization and cell motility through phosphorylation of cortactin.* J Biol Chem, 2010. **285**(24): p. 18672-83.
50. Jaggi, M., et al., *E-cadherin phosphorylation by protein kinase D1/protein kinase C{mu} is associated with altered cellular aggregation and motility in prostate cancer.* Cancer Res, 2005. **65**(2): p. 483-92.
51. Storz, P. and A. Toker, *Protein kinase D mediates a stress-induced NF-kappaB activation and survival pathway.* EMBO J, 2003. **22**(1): p. 109-20.
52. Asaithambi, A., et al., *Protein kinase D1 (PKD1) activation mediates a compensatory protective response during early stages of oxidative stress-induced neuronal degeneration.* Mol Neurodegener, 2011. **6**: p. 43.
53. Xiang, S.Y., et al., *PLCepsilon, PKD1, and SSH1L transduce RhoA signaling to protect mitochondria from oxidative stress in the heart.* Sci Signal, 2013. **6**(306): p. ra108.
54. Fielitz, J., et al., *Requirement of protein kinase D1 for pathological cardiac remodeling.* Proc Natl Acad Sci U S A, 2008. **105**(8): p. 3059-63.

55. Johannessen, M., et al., *Protein kinase D induces transcription through direct phosphorylation of the cAMP-response element-binding protein.* J Biol Chem, 2007. **282**(20): p. 14777-87.
56. Ozgen, N., et al., *Protein kinase D links Gq-coupled receptors to cAMP response element-binding protein (CREB)-Ser133 phosphorylation in the heart.* J Biol Chem, 2008. **283**(25): p. 17009-19.
57. Marklund, U., K. Lightfoot, and D. Cantrell, *Intracellular location and cell context-dependent function of protein kinase D.* Immunity, 2003. **19**(4): p. 491-501.
58. Ittner, A., et al., *Regulation of PTEN activity by p38delta-PKD1 signaling in neutrophils confers inflammatory responses in the lung.* J Exp Med, 2012. **209**(12): p. 2229-46.
59. Bard, F. and V. Malhotra, *The formation of TGN-to-plasma-membrane transport carriers.* Annu Rev Cell Dev Biol, 2006. **22**: p. 439-55.
60. Goginashvili, A., et al., *Insulin granules. Insulin secretory granules control autophagy in pancreatic beta cells.* Science, 2015. **347**(6224): p. 878-82.
61. Ferdaoussi, M., et al., *G protein-coupled receptor (GPR)40-dependent potentiation of insulin secretion in mouse islets is mediated by protein kinase D1.* Diabetologia, 2012. **55**(10): p. 2682-92.
62. Sundram, V., S.C. Chauhan, and M. Jaggi, *Emerging roles of protein kinase D1 in cancer.* Mol Cancer Res, 2011. **9**(8): p. 985-96.
63. Kim, M., et al., *Epigenetic inactivation of protein kinase D1 in gastric cancer and its role in gastric cancer cell migration and invasion.* Carcinogenesis, 2008. **29**(3): p. 629-37.
64. Durand, N., S. Borges, and P. Storz, *Functional and therapeutic significance of protein kinase D enzymes in invasive breast cancer.* Cell Mol Life Sci, 2015. **72**(22): p. 4369-82.
65. Du, C., et al., *Protein kinase D1 suppresses epithelial-to-mesenchymal transition through phosphorylation of snail.* Cancer Res, 2010. **70**(20): p. 7810-9.
66. Guha, S., et al., *Role of protein kinase D signaling in pancreatic cancer.* Biochem Pharmacol, 2010. **80**(12): p. 1946-54.
67. Harikumar, K.B., et al., *A novel small-molecule inhibitor of protein kinase D blocks pancreatic cancer growth in vitro and in vivo.* Mol Cancer Ther, 2010. **9**(5): p. 1136-46.
68. Locke, A.E., et al., *Genetic studies of body mass index yield new insights for obesity biology.* Nature, 2015. **518**(7538): p. 197-206.
69. Eguchi, J., et al., *Transcriptional control of adipose lipid handling by IRF4.* Cell Metab, 2011. **13**(3): p. 249-59.
70. Yvonne B. Sullivan1, D.E.H., Janaki Narahari1, Emily M. Anderson2, Anja Smith2 and Brian L. Webb1. *Importance of siRNA negative control selection: Evaluation of non-specific protein knockdown by negative control siRNA*. Poster]. Available from: http://dharmacon.gelifesciences.com/uploadedfiles/resources/sirna-negative-controls-poster.pdf.

71. *Basic siRNA Resuspension*. 2014; Available from: http://dharmacon.gelifesciences.com/uploadedfiles/resources/basic-sirna-resuspension-protocol.pdf.
72. Arsenijevic, T., et al., *Murine 3T3-L1 adipocyte cell differentiation model: validated reference genes for qPCR gene expression analysis.* PLoS One, 2012. **7**(5): p. e37517.
73. ATCC *ChemiCally-induCed differentiation of atCC® CL-173TM (3T3-L1) using single-Compo- nent CommerCially-available reagents*. **Tech Bulletin No. 9**.
74. Bastidas, O. *Cell Counting with Neubauer Chamber, Basic Hemocytometer Usage*. Available from: http://futurescienceleaders.org/protocols/files/2013/02/Cell-counting-Neubauer-chamber.pdf.
75. Kilroy, G., D.H. Burk, and Z.E. Floyd, *High efficiency lipid-based siRNA transfection of adipocytes in suspension.* PLoS One, 2009. **4**(9): p. e6940.
76. Lonza. *4D-NucleofectorTM Protocol for undifferentiated 3T3-L1 cells; For 4D-NucleofectorTM X Unit–Transfection in suspension; Mouse embryonal fibroblast; fibroblastoid cells*. 2013; Available from: http://bio.lonza.com/fileadmin/groups/marketing/Downloads/Protocols/Generated/Optimized_Protocol_358.pdf.
77. DiDonato, D. and D.L. Brasaemle, *Fixation methods for the study of lipid droplets by immunofluorescence microscopy.* J Histochem Cytochem, 2003. **51**(6): p. 773-80.
78. QIAGEN *QIAzol Lysis Reagent Quick-Start Protocol*. 2011.
79. Products, T.F.S.N. *Assessment of Nucleic Acid Purity*. T042 ‑ TECHNICAL BULLETIN NanoDrop Spectrophotometers 2011; Available from: http://nanodrop.com/Library/T042-NanoDrop-Spectrophotometers-Nucleic-Acid-Purity-Ratios.pdf.
80. Inc, T.F.S. *Real-time PCR Handbook*. 2014; Available from: http://www.lifetechnologies.com/content/dam/LifeTech/global/Forms/PDF/real-time-pcr-handbook.pdf.
81. Hui, K., et al., *The p38 MAPK-regulated PKD1/CREB/Bcl-2 pathway contributes to selenite-induced colorectal cancer cell apoptosis in vitro and in vivo.* Cancer Lett, 2014. **354**(1): p. 189-99.
82. Xie, L., et al., *Adiponectin and leptin are secreted through distinct trafficking pathways in adipocytes.* Biochim Biophys Acta, 2008. **1782**(2): p. 99-108.
83. Gnad, T., et al., *Adenosine activates brown adipose tissue and recruits beige adipocytes via A2A receptors.* Nature, 2014. **516**(7531): p. 395-9.
84. Garcia-Ruiz, E., et al., *The intake of high-fat diets induces the acquisition of brown adipocyte gene expression features in white adipose tissue.* Int J Obes (Lond), 2015. **39**(11): p. 1619-29.
85. Harms, M. and P. Seale, *Brown and beige fat: development, function and therapeutic potential.* Nat Med, 2013. **19**(10): p. 1252-63.
86. Li, J.Z., et al., *Cideb regulates diet-induced obesity, liver steatosis, and insulin sensitivity by controlling lipogenesis and fatty acid oxidation.* Diabetes, 2007. **56**(10): p. 2523-32.

87. Wu, J., et al., *Beige adipocytes are a distinct type of thermogenic fat cell in mouse and human.* Cell, 2012. **150**(2): p. 366-76.
88. Garcia, R.A., J.N. Roemmich, and K.J. Claycombe, *Evaluation of markers of beige adipocytes in white adipose tissue of the mouse.* Nutr Metab (Lond), 2016. **13**: p. 24.
89. Bartness, T.J. and C.K. Song, *Thematic review series: adipocyte biology. Sympathetic and sensory innervation of white adipose tissue.* J Lipid Res, 2007. **48**(8): p. 1655-72.
90. Jordan, J., et al., *Adrenergic responsiveness of adipose tissue lipolysis in autonomic failure.* Clin Auton Res, 2004. **14**(2): p. 80-3.
91. Wang, Y.-X., et al., *PPARdelta activates fat metabolism to prevent obesity.* Cell, 2003. **113**(4): p. 159–170.
92. Iglesias, J., et al., *PPARbeta/delta affects pancreatic beta cell mass and insulin secretion in mice.* J Clin Invest, 2012. **122**(11): p. 4105-17.
93. Mottillo, E.P., et al., *Lipolytic products activate peroxisome proliferator-activated receptor (PPAR) alpha and delta in brown adipocytes to match fatty acid oxidation with supply.* J Biol Chem, 2012. **287**(30): p. 25038-48.
94. Takahashi, S., et al., *Peroxisome proliferator-activated receptor delta (PPARdelta), a novel target site for drug discovery in metabolic syndrome.* Pharmacol Res, 2006. **53**(6): p. 501-7.
95. Puigserver, P. and B.M. Spiegelman, *Peroxisome proliferator-activated receptor-gamma coactivator 1 alpha (PGC-1 alpha): transcriptional coactivator and metabolic regulator.* Endocr Rev, 2003. **24**(1): p. 78-90.
96. Evans, R.M., G.D. Barish, and Y.X. Wang, *PPARs and the complex journey to obesity.* Nat Med, 2004. **10**(4): p. 355-61.
97. Mottillo, E.P. and J.G. Granneman, *Intracellular fatty acids suppress beta-adrenergic induction of PKA-targeted gene expression in white adipocytes.* Am J Physiol Endocrinol Metab, 2011. **301**(1): p. E122-31.
98. Ay, M., et al., *Molecular cloning, epigenetic regulation, and functional characterization of Prkd1 gene promoter in dopaminergic cell culture models of Parkinson's disease.* J Neurochem, 2015. **135**(2): p. 402-15.
99. Borges, S., et al., *Pharmacologic reversion of epigenetic silencing of the PRKD1 promoter blocks breast tumor cell invasion and metastasis.* Breast Cancer Res, 2013. **15**(2): p. R66.
100. Baker, R.G., M.S. Hayden, and S. Ghosh, *NF-kappaB, inflammation, and metabolic disease.* Cell Metab, 2011. **13**(1): p. 11-22.
101. Jung, K.J., et al., *Effect of short term calorie restriction on pro-inflammatory NF-kB and AP-1 in aged rat kidney.* Inflamm Res, 2009. **58**(3): p. 143-50.
102. Harrison, B.C., et al., *Regulation of cardiac stress signaling by protein kinase d1.* Mol Cell Biol, 2006. **26**(10): p. 3875-88.
103. Yamauchi, T., et al., *The mechanisms by which both heterozygous peroxisome proliferator-activated receptor gamma (PPARgamma) deficiency and PPARgamma agonist improve insulin resistance.* J Biol Chem, 2001. **276**(44): p. 41245-54.

104. Doppler, H., et al., *The PRKD1 promoter is a target of the KRas-NF-kappaB pathway in pancreatic cancer.* Sci Rep, 2016. **6**: p. 33758.
105. Chiang, S.H., et al., *The protein kinase IKKepsilon regulates energy balance in obese mice.* Cell, 2009. **138**(5): p. 961-75.
106. Weisberg, S.P., et al., *Obesity is associated with macrophage accumulation in adipose tissue.* J Clin Invest, 2003. **112**(12): p. 1796-808.
107. Alkhouri, N., et al., *Adipocyte apoptosis, a link between obesity, insulin resistance, and hepatic steatosis.* J Biol Chem, 2010. **285**(5): p. 3428-38.
108. Keuper, M., et al., *An inflammatory micro-environment promotes human adipocyte apoptosis.* Mol Cell Endocrinol, 2011. **339**(1-2): p. 105-13.
109. Rybin, V.O., et al., *Regulatory domain determinants that control PKD1 activity.* J Biol Chem, 2012. **287**(27): p. 22609-15.
110. Endo, K., et al., *Proteolytic cleavage and activation of protein kinase C [micro] by caspase-3 in the apoptotic response of cells to 1-beta -D-arabinofuranosylcytosine and other genotoxic agents.* J Biol Chem, 2000. **275**(24): p. 18476-81.
111. Orban, T.I. and E. Olah, *Emerging roles of BRCA1 alternative splicing.* Mol Pathol, 2003. **56**(4): p. 191-7.
112. Ellisen, L.W., *Regulation of gene expression by WT1 in development and tumorigenesis.* Int J Hematol, 2002. **76**(2): p. 110-6.
113. Coughlan, K.A., et al., *PKD1 Inhibits AMPKalpha2 through Phosphorylation of Serine 491 and Impairs Insulin Signaling in Skeletal Muscle Cells.* J Biol Chem, 2016. **291**(11): p. 5664-75.
114. Bijland, S., S.J. Mancini, and I.P. Salt, *Role of AMP-activated protein kinase in adipose tissue metabolism and inflammation.* Clin Sci (Lond), 2013. **124**(8): p. 491-507.
115. Brasaemle, D.L., et al., *The lipolytic stimulation of 3T3-L1 adipocytes promotes the translocation of hormone-sensitive lipase to the surfaces of lipid storage droplets.* Biochim Biophys Acta, 2000. **1483**(2): p. 251-62.
116. Seale, P., et al., *Prdm16 determines the thermogenic program of subcutaneous white adipose tissue in mice.* J Clin Invest, 2011. **121**(1): p. 96-105.
117. Wilson-Fritch, L., et al., *Mitochondrial remodeling in adipose tissue associated with obesity and treatment with rosiglitazone.* J Clin Invest, 2004. **114**(9): p. 1281-9.
118. Choi, S.S., J. Park, and J.H. Choi, *Revisiting PPARgamma as a target for the treatment of metabolic disorders.* BMB Rep, 2014. **47**(11): p. 599-608.
119. Bundesärztekammer, K.r.B., Arbeitsgemeinschaft der Wissenschaftlichen Medizinischen Fachgesellschaften *Nationale Versorgungs Leitlinie Therapie des Typ-2-Diabetes Langfassung*. 2014.

9 Table of figures

10 Appendix

10.1 Abbreviations

ATGL	Adipose triglyceride lipase
AMPK	AMP-activated protein kinase
BAT	Brown adipose tissue
BMI	Body mass index
ca	Constitutive active
Cont.	Control
CRD	Cysteine-rich domain
CREB	cAMP-response element-binding protein
DAG	Diacylglycerol
DM	Diabetes mellitus
epiWAT	Epigonadal white adipose tissue
FCS	Calf bovine serum, iron fortifierd
FBS	Fetal bovine serum
FFA	Free fatty acids
GPCR	G-protein coupled receptor
HDAC	Histone deacetylases
HFD	High fat diet
HSL	Hormone-sensitive lipase
IDF	International Diabetes Federation
Kd	Kinase dead
MGL	Monoacylgycerol lipase
mRNA	Messenger RNA
ND	Normal rodents chow diet
NF-κB	Nucelar factor κB
PGC-1α	Transcriptional coactivator of PPARγ

PH	Pleckstrin homology
PKC	Protein kinase C
PKD	Protein kinase D
PKD1	Protein kinase D 1
PLC	Phosolipase C
pSer-744, -748, -916	Phosphorylated Serine-744, -748, -916
PPAR	Peroxisome proliferator-acitvated receptor
qRT-PCR	Quantitative real-time polymerase chain reaction
siATGL	siRNA targeting ATGL
siCtrl	non-targeting siRNA
siRNA	Small interfering RNA
SNP	Single nucleotide polymorphism
subWAT	Subcutaneous white adipose tissue
T2DM	Type 2 diabetes mellitus
TG	Triacylglyceride
TGN	Trans-Golgi network
TKR	Tyrosine-kinase receptor
WAT	White adipose tissue
WHO	World Health Organization
wt	wildtype
UCP-1	Uncoupling protein-1

10.2 Acknowledgements

First, I would like to thank my supervisor Dr. Grzegorz Sumara for giving me the opportunity to work on this study and conduct experiments in his laboratory at Rudolf-Virchow-Zentrum in Würzburg. Dr. Grzegorz Sumara supported me with his scientific experience, inspiring discussions, and leadership in his research group. The material and equipment for this study was kindly provided by G. Sumara research group.

I thank Mona Löffler for instructing and supervising me throughout the scientific work. M. Löfflers valuable feedback and conversations were of great support. Also, I would like to thank the team of G. Sumara research group for constructive advice and restoring breaks with room for chats, jokes and laughter (Mona Löffler, Alexander Mayer, Rabih El-Merhabi, Jonathan Trujillo Viera).

I am very grateful to Prof. Dr. Antje Gohla from the Institute of Pharmacology in Würzburg for guiding me in this work and being member of my supervision committee. Also, I thank Prof. Dr. Fassnacht for membership in my supervision committee.

Furthermore, I would like to give my sincere gratitude to Gisela Slotta and Hannah Thieron for valuable suggestions and encouragement. Of course, this work would not have been possible without unlimited and kind support of my family.

I thank my fellows and friends who have encouraged me throughout my academic studies and life. This time would not have been nearly as memorable and extraordinary if we had not gone through it together.

Finally, I am very grateful to David Thiemann for being patient with me and supporting me in multiple ways.